Geophys. J. Int. (2002) **149,** 698–723

On strike-slip faulting in layered media

Maurizio Bonafede, Beatrice Parenti and Eleonora Rivalta

Department of Physics, University of Bologna, viale Berti-Pichat 8, 40127 *Bologna, Italy. E-mail: bonafede@ibogfs.df.unibo.it*

Accepted 2001 December 15. Received 2001 December 15; in original form 2000 November 13

SUMMARY

We study the effects of structural inhomogeneities on the stress and displacement fields induced by strike-slip faults in layered media. An elastic medium is considered, made up of an upper layer bounded by a free surface and welded to a lower half-space characterized by different elastic parameters. Shear cracks with assigned stress drop are employed as mathematical models of strike-slip faults, which are assumed to be vertical and planar. If the crack is entirely embedded within the lower medium (case A), a Cauchy-kernel integral equation is obtained, which is solved by employing an expansion of the dislocation density in Chebyshev polynomials. If the crack is within the lower medium but it terminates at the interface (case B), a generalized Cauchy singularity appears in the integral kernel. This singularity affects the singular behaviour of the dislocation density at the crack tip touching the interface. Finally, the case of a crack crossing the interface is considered (case C). The crack is split into two interacting sections, each placed in a homogeneous medium and both open at the interface. Two coupled generalized Cauchy equations are obtained and solved for the dislocation density distribution of each crack section. An asymptotic study near the intersection between the crack and the interface shows that the dislocation densities for each crack section are bounded at the interface, where a jump discontinuity is present. As a corollary, the stress drop must be discontinuous at the interface, with a jump proportional to the rigidity contrast between the adjoining media. This finding is shown to have important implications for the development of geometrical complexities within transform fault zones: planar strike-slip faults cutting across layer discontinuities with arbitrary stress drop values are shown to be admissible only if the interface between different layers becomes unwelded during the earthquake at the crack/interface junction. Planar strike-slip faulting may take place only in mature transform zones, where a repetitive earthquake cycle has already developed, if the rheology is perfectly elastic. Otherwise, the fault cannot be planar: we infer that strike-slip faulting at depth is plausibly accompanied by en-echelon surface breaks in a shallow sedimentary layer (where the stress drop is lower than prescribed by the discontinuity condition), while ductile deformation (or steady sliding) at depth may be accommodated by multiple fault branching or by antithetic faulting in the upper brittle layer (endowed with lower rigidity but higher stress).

Key words: crack model, layered media, strike-slip faults, transform boundaries.

INTRODUCTION

Recent developments in the field of fault mechanics show that a major insight can be gained on the mechanisms of fault instability by appropriate modelling of the stress field induced by an earthquake in the surrounding areas (e.g. Stein *et al.* 1992; King *et al.* 1994), employing the modified Coulomb failure criterion. An increase of the deviatoric stress, a decrease of normal stress (e.g. Kagan & Jackson 1998; Perfettini *et al.* 1999) and an increase of pore pressure can destabilize suitably oriented faults after an earthquake in their proximity. Reverse changes bring faults to a state of greater stability, giving rise to the concept of stress shadows (e.g. Harris & Simpson 1998). The more advanced 'rate and state-dependent friction laws' yield physically sound explanations of the space–time evolution of aftershock sequences and of triggered seismicity events (e.g. Gomberg *et al.* 1998). These findings clearly have important implications for the assessment of seismic hazard (e.g. Harris 1998; Nalbant *et al.* 1998).

Static dislocation models in the antiplane configuration are generally employed to model the stress and deformation pattern around faults. In this framework, a fairly complete set of analytical solutions has been worked out for rectangular dislocation surfaces, with uniform slip,

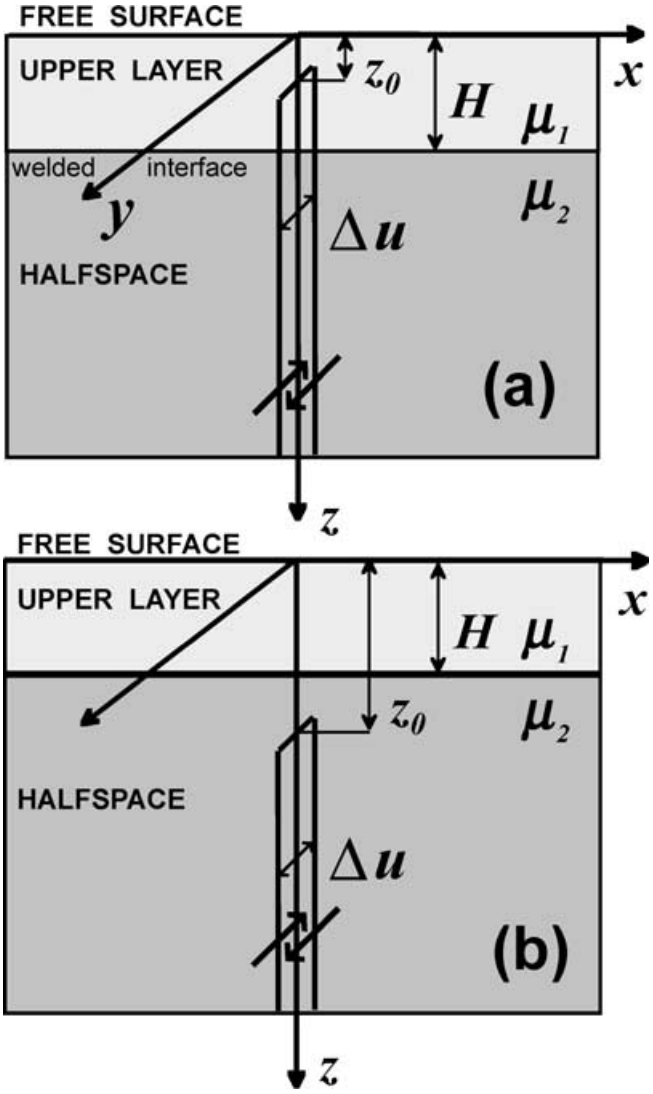

Figure 1. The layer 1 ($0 < z < H$) is welded to the half-space 2 ($z > H$). Two elementary screw dislocations are shown. The Burgers vector Δu is in y-direction. In (a) the dislocation plane cuts across the interface between layer 1 and half-space 2; in (b) it is contained within half-space 2.

in homogeneous elastic half-spaces (e.g. Okada 1992). Several solutions exist in layered media, but these are generally restricted to point sources (Singh 1970; Rundle 1978; Roth 1990; Ben-Zion 1990; Kumari *et al.* 1992; Tinti & Armigliato 1998). Dislocation point sources have also been considered in spherically layered (e.g. Pollitz 1992; Pollitz & Sacks 1996) and self-gravitating Earth models (Piersanti *et al.* 1995, 1997) in order to study the far-field effects of large earthquakes; when point source distributions are employed to model an extended fault, severe convergence problems are, however, met in the near field (see, e.g. Fig. 1 in Antonioli *et al.* 1998). The mathematical motivation for this failure is in the non-integrable singularity of the stress field and its derivatives that are present at each point source (to this end, the same considerations apply which are given on pp. 424–428 in Bonafede & Rivalta 1999a, for tensile dislocations). Several schemes for obtaining numerical solutions of rectangular shear dislocations in layered media are also available (e.g. Rundle 1978; Savage 1987, 1998; Ma & Kusznir 1994; Singh *et al.* 1993; Rani *et al.* 1995), but these generally assume a constant slip discontinuity over the dislocation surface and cannot be readily employed in crack models of faults, in which the stress drop is assigned.

The purpose of the present paper is to study the stress changes induced by faulting in proximity of layer discontinuities, by developing accurate solutions to antiplane (mode III) crack problems in horizontally layered elastic media. In a crack model it is assumed that the stress drop is assigned over the crack plane; we shall study analytically the singularities appearing at the intersection between the crack plane and the interface between different media. To this end, some non-crucial simplifying assumptions are made: an antiplane (2-D) strain configuration is employed, an infinite (along-strike) fault surface is considered, vertically dipping across a horizontally layered medium: the medium consists of an upper layer, bounded by a free surface and welded along its base to a half-space with different rigidity. Three cases must be considered: the crack is entirely within the lower half-space (case A); the upper crack tip touches the interface between the two media (case B); the crack extends across the interface (case C). The case of a crack embedded within the upper layer can be solved in much the same way as cases B and A, according to whether it terminates at the interface or not.

THE SHEAR CRACK IN A LAYERED HALF-SPACE

Consider a medium made up of an elastic layer: $0 \leq z \leq H$ with rigidity μ_1 and Poisson ratio ν_1, with a free surface in $z = 0$ and welded in $z = H$ to a lower half-space: $z \geq H$ with elastic parameters μ_2, ν_2 (Fig. 1).

An antiplane strain configuration is considered, in which the only non-vanishing component of the displacement field is $u_y(x, z)$, which is independent of the coordinate y. The analytical solutions for an elementary screw dislocation with constant Burgers vector in such a medium are given by Rybicki (1971); in the reference system employed here the Burgers vector is in the y-direction and the dislocation line is defined by $(z = z_0) \wedge (x = 0)$.

Solutions are given for the non-vanishing components of the stress field $(\sigma_{xy}, \sigma_{yz})$ and of the displacement field u_y, according to whether $z_0 < H$ or $z_0 > H$. The elementary solutions will be written, from now on, as $\sigma_{xy}^{\mathrm{el}}(x, z; z_0)$, $u_y^{\mathrm{el}}(x, z; z_0)$, etc. These expressions denote effects induced in (x, z) by a dislocation surface $(z > z_0) \wedge (x = 0)$ with a unit Burgers vector in the y-direction.

Employing suitable superpositions of elementary solutions, a crack model can be obtained, in which the stress drop over the fault surface is assigned (instead of the slip). The crack domain will be assumed to be the strip $(c - \ell \leq z \leq c + \ell) \wedge (x = 0)$, where ℓ and c denote, respectively, the crack half-length the depth of its midpoint. Over the crack domain the equilibrium equation is

$$\sigma_{xy}^{0}(x = 0, z) + \sigma_{xy}^{\mathrm{c}}(x = 0, z) = \sigma_{xy}^{\mathrm{r}}(x = 0, z) \qquad c - \ell < z < c + \ell, \tag{1}$$

where σ_{xy}^{0} denotes the stress present over the crack domain before slip occurrence, σ_{xy}^{c} represents the stress induced by crack slip and σ_{xy}^{r} is the residual stress field after slip occurrence.

Employing a continuous distribution of elementary dislocations with dislocation lines contained in the interval $c - \ell < z_0 < c + \ell$, the previous equation becomes

$$-\Delta\sigma(z) = \int_{c-\ell}^{c+\ell} \sigma_{xy}^{\mathrm{el}}(0, z; z_0)\rho(z_0)\, dz_0, \quad c - \ell < z < c + \ell, \tag{2}$$

where the integral is evaluated in the principal-value sense (since $\sigma_{xy}^{\mathrm{el}}$ has a Cauchy-type singularity at $z = z_0, x = 0$), $\Delta\sigma(z) = \sigma_{xy}^{0} - \sigma_{xy}^{\mathrm{r}}$ is the 'stress drop' and ρ denotes the unknown dislocation density distribution, which is defined through the displacement discontinuity over the crack plane $\Delta u(z) = u_y(0^+, z) - u_y(0^-, z)$ in the following way:

$$\rho(z_0) = \left[\frac{\partial \Delta u(z)}{\partial z}\right]_{z=z_0}. \tag{3}$$

From eq. (3) we obtain

$$\Delta u(z) = \int_{c-\ell}^{z} \rho(z_0)\, dz_0 + C, \tag{4}$$

where C is a constant. Requiring the condition of crack closure at the upper tip $(z = c - \ell)$ it follows that $C = 0$. If the stress drop $\Delta\sigma$ is assigned, eq. (2) is an integral equation for ρ. The integral kernel $\sigma_{xy}^{\mathrm{el}}(0, z; z_0)$ in eq. (2) was obtained by Rybicki (1971) according to four possible cases:

I-1: $z < H, z_0 < H$. Stress in the upper layer 1 caused by an elementary dislocation in the same layer 1, denoted in the following as σ_1^{I}.
I-2: $z > H, z_0 < H$. Stress in the lower half-space 2 caused by an elementary dislocation in layer 1, denoted as σ_2^{I}.
II-1: $z < H, z_0 > H$. Stress in layer 1 caused by a dislocation in half-space 2, denoted as σ_1^{II}.
II-2: $z > H, z_0 > H$. Stress in half-space 2 caused by a dislocation in half-space 2, denoted as σ_2^{II}.

In a similar way we shall denote the elementary displacement field u_y^{el} as $u_1^{\mathrm{I}}, u_2^{\mathrm{I}}, u_1^{\mathrm{II}}, u_2^{\mathrm{II}}$, respectively. Rybicki's solution for case I was written only over the free surface $z = 0$. In order to have solutions valid throughout the layered half-space, we adapted to our problem a method of solution based on the Galerkin vector scheme (Fung 1965), described in detail by Bonafede & Rivalta (1999b), for the tensile dislocation problem. Our solutions, obtained following this method, are coincident with Rybicki's results for all the cases considered. The complete set of solutions for the displacement field is reproduced below for ease of reference. According to the four cases mentioned, the elementary solution u_y^{el} (for a unit Burgers vector) is given by

$$u_1^{\mathrm{I}}(x, z; z_0) = \frac{1}{2\pi}\left[\Phi(x, z - z_0) + \arctan\frac{x}{z + z_0} - \sum_{n=1}^{\infty}\Gamma^n\left(\arctan\frac{x}{z - z_0 + 2nH} + \arctan\frac{x}{z - z_0 - 2nH}\right.\right.$$
$$\left.\left. - \arctan\frac{x}{z + z_0 + 2nH} - \arctan\frac{x}{z + z_0 - 2nH}\right)\right] \tag{5}$$

$$u_2^{\mathrm{I}}(x,z;z_0)=\frac{1}{2\pi}\left[\Phi(x,z-z_0)-\Gamma\arctan\frac{x}{z-z_0}\right]$$
$$-\frac{1}{\pi(1+m)}\left[\sum_{n=1}^{\infty}\Gamma^n\left(\arctan\frac{x}{z-z_0+2nH}-\arctan\frac{x}{z+z_0+2nH}\right)-\arctan\frac{x}{z+z_0}\right] \tag{6}$$

$$u_1^{\mathrm{II}}(x,z;z_0)=\frac{1}{2\pi}\left[\Phi(x,z-z_0)+\Gamma\arctan\frac{x}{z-z_0}\right]+\frac{1}{\pi}\frac{m}{m+1}\left(\sum_{n=0}^{\infty}\Gamma^n\arctan\frac{x}{z+z_0+2nH}+\sum_{n=1}^{\infty}\Gamma^n\arctan\frac{x}{z_0-z+2nH}\right) \tag{7}$$

$$u_2^{\mathrm{II}}(x,z;z_0)=\frac{1}{2\pi}\left[\Phi(x,z-z_0)-\Gamma\arctan\frac{x}{z+z_0-2H}+\frac{4m}{(1+m)^2}\sum_{n=0}^{\infty}\Gamma^n\arctan\frac{x}{z_0+z+2nH}\right], \tag{8}$$

where $m=\mu_2/\mu_1$, $\Gamma=(\frac{1-m}{1+m})$ and the function $\Phi(x,z)$ is defined as

$$\Phi(x,z)=\begin{cases}\dfrac{\pi}{2}+\arctan\dfrac{z}{x} & \text{if}\quad x>0\\[2ex] -\dfrac{\pi}{2}+\arctan\dfrac{z}{x} & \text{if}\quad x<0.\end{cases}$$

Suitable superpositions of such solutions have been often employed to represent strike-slip faults in elastic and viscoelastic layered media. Elementary stress components can be easily obtained differentiating the previous equations according to the constitutive relationships of linear elasticity; only the two components $\sigma_{xy}^{\mathrm{el}}$ and $\sigma_{yz}^{\mathrm{el}}$ are non-vanishing:

$$\sigma_{xy}^{\mathrm{el}}(x,z;z_0)=\mu\frac{\partial u_y^{\mathrm{el}}}{\partial x},\quad \sigma_{yz}^{\mathrm{el}}(x,z;z_0)=\mu\frac{\partial u_y^{\mathrm{el}}}{\partial z}. \tag{9}$$

In the previous equation, if $z<H$ then $\mu=\mu_1$ and $u^{\mathrm{el}}=u_1^{\mathrm{I}}$, or $u^{\mathrm{el}}=u_1^{\mathrm{II}}$ according to whether $z_0<H$ or $z_0>H$, respectively; if $z>H$ then $\mu=\mu_2$ and $u^{\mathrm{el}}=u_2^{\mathrm{I}}$, or $u^{\mathrm{el}}=u_2^{\mathrm{II}}$ according to whether $z_0<H$ or $z_0>H$, respectively. In the present paper we shall be mainly interested in the expressions of the stress component $\sigma_{xy}^{\mathrm{el}}(0,z;z_0)$ on the dislocation plane $x=0$, which are reported below according to the four different cases considered above (the subscripts xy and the argument $x=0$ are omitted):

$$\sigma_1^{\mathrm{I}}(z;z_0)=-\frac{\mu_1}{2\pi}\left[\frac{1}{z-z_0}-\frac{1}{z+z_0}+\sum_{n=1}^{\infty}\Gamma^n\left(\frac{1}{z-z_0+2nH}+\frac{1}{z-z_0-2nH}-\frac{1}{z+z_0+2nH}-\frac{1}{z+z_0-2nH}\right)\right] \tag{10}$$

$$\sigma_2^{\mathrm{I}}(z;z_0)=-\frac{\mu_2}{\pi(1+m)}\sum_{n=0}^{\infty}\Gamma^n\left(\frac{1}{z-z_0+2nH}-\frac{1}{z+z_0+2nH}\right) \tag{11}$$

$$\sigma_1^{\mathrm{II}}(z;z_0)=\frac{m\mu_1}{\pi(1+m)}\sum_{n=0}^{\infty}\Gamma^n\left(\frac{1}{z_0+z+2nH}+\frac{1}{z_0-z+2nH}\right) \tag{12}$$

$$\sigma_2^{\mathrm{II}}(z;z_0)=-\frac{\mu_2}{2\pi}\left[\frac{1}{z-z_0}+\Gamma\frac{1}{z+z_0-2H}-\frac{4m}{(1+m)^2}\sum_{n=0}^{\infty}\Gamma^n\frac{1}{z_0+z+2nH}\right]. \tag{13}$$

Recall that the previous expressions for displacement and stress components are referred to a unit Burgers vector and accordingly have dimensions [m m^{-1}] and [Pa m^{-1}], respectively. Inserting the previous expressions for $\sigma_{xy}^{\mathrm{el}}$ in eq. (2), the equilibrium equation is obtained for a crack in the layered half-space; three cases will be considered (Fig. 2).

Case A: $H<c-\ell<c+\ell$. The crack is entirely embedded in the lower medium. Inserting $\sigma_2^{\mathrm{II}}(z;z_0)$ (for $\sigma_{xy}^{\mathrm{el}}(z;z_0)$) in eq. (2) only a Cauchy singularity is provided from the first term of eq. (13) when $z=z_0$. The principal value of the integral is to be considered (Fig. 2A).

Case B: $H=c-\ell<c+\ell$. The upper tip of the crack is at the interface between the two media. Another singularity appears in the second term of eq. (13) for $z=z_0=H$; a generalized Cauchy kernel is obtained. As in case A, singular integrals must be evaluated in the principal-value sense (Fig. 2B).

Case C: $c-\ell<H<c+\ell$. The crack crosses the interface and in addition to the Cauchy singularity in $z=z_0$, the integral kernel contains further singularities at $z=z_0=H$ (Fig. 2C). We consider the crack as split into two interacting open cracks, each embedded in a homogeneous medium.

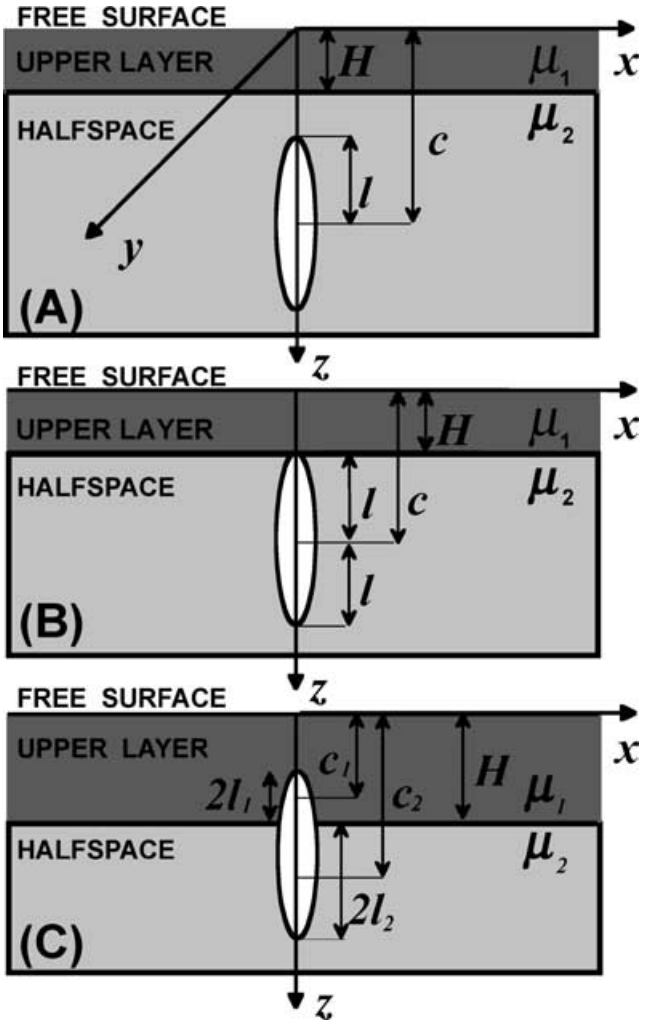

Figure 2. Three cases of a crack in the layered half-space. Crack slip is in y-direction and the x-axis is normal to the crack plane. In case A the crack is embedded within half-space 2, ℓ is the half-length of the crack and c is its midpoint. In case B the crack touches the interface, $z = H$ and $c = \ell + H$. In case C two interacting open cracks, with mid points c_1, c_2 and half-lengths ℓ_1, ℓ_2 are shown. Their common tip is in $z = H$.

In case C, the resulting coupled equilibrium equations of generalized Cauchy type are

$$\begin{aligned} -\Delta\sigma(z) &= \int_{H-2\ell_1}^{H} \sigma_1^{\mathrm{I}}(z;z_0)\rho_1(z_0)\,dz_0 + \int_{H}^{H+2\ell_2} \sigma_1^{\mathrm{II}}(z;z_0)\rho_2(z_0)\,dz_0 \quad H-2\ell_1 < z < H \\ -\Delta\sigma(z) &= \int_{H-2\ell_1}^{H} \sigma_2^{\mathrm{I}}(z;z_0)\rho_1(z_0)\,dz_0 + \int_{H}^{H+2\ell_2} \sigma_2^{\mathrm{II}}(z;z_0)\rho_2(z_0)\,dz_0 \quad H < z < H+2\ell_2, \end{aligned} \tag{14}$$

where ℓ_1 and ℓ_2 are the half-lengths of the two interacting crack sections and ρ_1 and ρ_2 represent their dislocation density distributions (Fig. 2C). The overall density is simply $\rho(z_0) = \rho_1(z_0)$ if $H - 2\ell_1 < z_0 < H$, while $\rho(z_0) = \rho_2(z_0)$ if $H < z_0 < H + 2\ell_2$.

Once the dislocation density ρ is known, the solution of a crack problem is simply obtained by a superposition of elementary solutions; for instance, if f^{el} denotes any elementary component of displacement or stress, the crack solution in case A or B is given by

$$f^{\mathrm{c}}(x,z) = \int_{c-\ell}^{c+\ell} f^{\mathrm{el}}(x,z;z_0)\rho(z_0)\,dz_0 \tag{15}$$

and by a sum of similar expressions in case C,

$$f^{\mathrm{c}}(x,z) = \int_{c_1-\ell_1}^{c_1+\ell_1} f^{\mathrm{el}}(x,z;z_0)\rho_1(z_0)\,dz_0 + \int_{c_2-\ell_2}^{c_2+\ell_2} f^{\mathrm{el}}(x,z;z_0)\rho_2(z_0)\,dz_0. \tag{16}$$

CASE A: CRACK EMBEDDED IN HALF-SPACE 2

First, we consider the simpler case of a crack entirely embedded in the lower medium (Fig. 2A). If the stress drop $\Delta\sigma$ is assigned over the crack domain, $H < c - \ell \le z \le c + \ell$, the equilibrium equation (2) can be written conveniently as

$$-\Delta\sigma(\ell\xi + c) = \ell \int_{-1}^{1} \sigma_2^{\mathrm{II}}(\ell\xi + c; \ell\xi' + c)\rho(\ell\xi' + c)\, d\xi' = \frac{\mu_2}{2\pi}\left[\int_{-1}^{1} \frac{\rho(\ell\xi' + c)}{\xi' - \xi}\, d\xi' + \int_{-1}^{1} \mathcal{R}_2^{\mathrm{II}}(\xi, \xi')\rho(\ell\xi' + c)\, d\xi'\right], \quad |\xi| < 1, \tag{17}$$

where the first integral within brackets must be evaluated in the principal-value sense and $\mathcal{R}_2^{\mathrm{II}}$ is the regular (Fredholm) integral kernel

$$\mathcal{R}_2^{\mathrm{II}}(\xi, \xi') = -\Gamma \frac{1}{\xi + \xi' + 2(\lambda - h)} + \frac{4m}{(1+m)^2} \sum_{n=0}^{\infty} \Gamma^n \frac{1}{\xi + \xi' + 2(\lambda + nh)} \tag{18}$$

the non-dimensional variables ξ, ξ' and parameters λ, h have been introduced:

$$\xi = (z - c)/\ell, \quad \xi' = (z_0 - c)/\ell, \quad \eta = x/\ell, \quad \lambda = c/\ell, \quad h = H/\ell. \tag{19}$$

In the following we shall employ the shorthand notation $\rho(\xi')$ and $\Delta\sigma(\xi)$ for $\rho(\ell\xi' + c)$ and $\Delta\sigma(\ell\xi + c)$. The unknown dislocation density distribution $\rho(\xi')$ can be split into the product of a singular factor $S(\xi')$ times a bounded factor $R(\xi')$ with $R(\pm 1) \neq 0$:

$$\rho(\xi') = (1 - \xi')^a (1 + \xi')^b R(\xi'), \tag{20}$$

where $a = b = -1/2$. According to Muskhelishvili (1953) this square-root singularity is required to provide finite $\Delta\sigma$ values within crack tips. If the bounded factor $R(\xi')$ is continuous, it can be expanded in a uniformly convergent series of Chebyshev polynomials of the first kind $T_k(\cos\theta) = \cos k\theta$ (Abramowitz & Stegun 1964; Bonafede *et al.* 1985) so that

$$\rho(\xi') = \frac{1}{\sqrt{1 - \xi'^2}} \sum_{k=0}^{\infty} \alpha_k T_k(\xi'). \tag{21}$$

Solving the equilibrium equation is then reduced to evaluating the unknown coefficients α_k.

One important property of Chebyshev polynomials, which is employed in the solution of the equilibrium equation (17), is the following principal-value integral:

$$\int_{-1}^{1} \frac{T_k(\xi')}{\xi' - \xi} \frac{d\xi'}{\sqrt{1 - \xi'^2}} = \begin{cases} \pi U_{k-1}(\xi) & \text{if} \quad k \ge 1 \\ 0 & \text{if} \quad k = 0, \end{cases} \quad |\xi| < 1, \tag{22}$$

where $U_k(\cos\theta) = \frac{\sin(k+1)\theta}{\sin\theta}$ are Chebyshev polynomials of the second kind. The condition of vanishing slip at crack tips $\Delta u(c \pm \ell) = 0$ imposes that $\alpha_0 = 0$ (obtained after inserting eq. 21 into eq. 4). Substituting the expansion (21) in eq. (17) and using eq. (22) the equilibrium equation becomes

$$-\Delta\sigma(\xi) = \frac{\mu_2}{2} \sum_{k=1}^{\infty} \alpha_k U_{k-1}(\xi) + \frac{\mu_2}{2\pi} \sum_{k=1}^{\infty} \alpha_k \mathcal{R}_k(\xi), \tag{23}$$

where

$$\mathcal{R}_k(\xi) = \int_{-1}^{1} \frac{T_k(\xi')}{\sqrt{1 - \xi'^2}} \mathcal{R}_2^{\mathrm{II}}(\xi, \xi')\, d\xi'.$$

Method of solution

If we multiply both sides of eq. (23) by the factor $U_i(\xi)\sqrt{1 - \xi^2}$ and integrate in $d\xi$ over the interval $(-1, 1)$ we obtain

$$\frac{\pi}{2}\sigma_i = -\mu_2 \frac{\pi}{4} \sum_{k=1}^{\infty} \alpha_k \delta_{i(k-1)} + \frac{\mu_2}{2\pi}\Gamma \sum_{k=1}^{\infty} \alpha_k I_1(k, i) - \frac{\mu_2}{\pi} \frac{2m}{(1+m)^2} \sum_{k=1}^{\infty} \alpha_k \sum_{n=0}^{\infty} \Gamma^n I_2(k, i, n), \tag{24}$$

where

$$I_1(k, i) = \int_{-1}^{1} d\xi\, U_i(\xi)\sqrt{1 - \xi^2} \left[\int_{-1}^{1} \frac{T_k(\xi')}{\xi + \xi' + 2(\lambda - h)} \frac{d\xi'}{\sqrt{1 - \xi'^2}}\right] \tag{25}$$

$$I_2(k, i, n) = \int_{-1}^{1} d\xi\, U_i(\xi)\sqrt{1 - \xi^2} \left[\int_{-1}^{1} \frac{T_k(\xi')}{\xi + \xi' + 2(\lambda + nh)} \frac{d\xi'}{\sqrt{1 - \xi'^2}}\right] \tag{26}$$

$$\frac{\pi}{2}\sigma_i = \int_{-1}^{1} \Delta\sigma(\xi) U_i(\xi)\sqrt{1-\xi^2}\, d\xi. \tag{27}$$

Integrals with respect to ξ' in $I_1(k,i)$, $I_2(k,i,n)$ are computed analytically in Appendix A, while the remaining integrals with respect to ξ can be computed efficiently and accurately employing a globally adaptive scheme for oscillatory weighted functions.

If we assume that $\Delta\sigma$ is constant and let $l = i+1$, we obtain

$$\Delta\sigma\,\delta_{l1} = \sum_{k=1}^{\infty} G_{lk}\alpha_k \quad l = 1, 2\ldots, \tag{28}$$

where

$$G_{lk} = -\frac{\mu_2}{2}\delta_{lk} + \frac{\mu_2}{\pi^2}\Gamma I_1(k, l-1) - \frac{\mu_2}{\pi^2}\frac{4m}{(1+m)^2}\sum_{n=0}^{\infty}\Gamma^n I_2(k, l-1, n). \tag{29}$$

This is an infinite-dimensional linear system for the expansion coefficients α_k; an approximate solution can be obtained if we use a truncation, to a finite order K, of the expansion (21) for $\rho(\xi')$. In order to compute the matrix elements G_{lk} we must also truncate the series in n (the third term of eq. 29), which represents the contribution of infinite 'mirror dislocations'. Let us define $\tilde{\rho}(\xi')$ as the truncated expansion of $\rho(\xi')$ and $\tilde{G}_{lk}$ the $K \times K$ matrix obtained by truncating the sum in eq. (29) to $n \leq N$. The resulting linear system to be solved is

$$\begin{aligned} &\tilde{\alpha}_0 = 0 \\ &\tilde{\alpha}_k = \Delta\sigma\,\tilde{G}_{kl}^{-1}\delta_{l1} \quad k, l = 1, 2, \ldots, K. \end{aligned} \tag{30}$$

Note that $\tilde{\alpha}_0 = 0$ is imposed separately, from the crack closure assumption; without this supplementary condition the problem would yield infinite solutions. Once the coefficients $\tilde{\alpha}_k$ have been computed, all the components of the stress and displacement fields can be evaluated as a superposition of elementary contributions, such as

$$\tilde{u}_{yi}(x,z) = \ell\sum_{k=1}^{K}\tilde{\alpha}_k\int_{-1}^{1} u_{yi}^{\mathrm{II}}(\ell\xi + c, \ell\xi' + c, \ell\eta)\frac{T_k(\xi')}{\sqrt{1-\xi'^2}}\, d\xi' \tag{31}$$

$$\tilde{\sigma}_{xyi}(x,z) = \ell\sum_{k=1}^{K}\tilde{\alpha}_k\int_{-1}^{1} \sigma_{xyi}^{\mathrm{II}}(\ell\xi + c, \ell\xi' + c, \ell\eta)\frac{T_k(\xi')}{\sqrt{1-\xi'^2}}\, d\xi' \tag{32}$$

$$\tilde{\sigma}_{yzi}(x,z) = \ell\sum_{k=1}^{K}\tilde{\alpha}_k\int_{-1}^{1} \sigma_{yzi}^{\mathrm{II}}(\ell\xi + c, \ell\xi' + c, \ell\eta)\frac{T_k(\xi')}{\sqrt{1-\xi'^2}}\, d\xi', \tag{33}$$

where $i = 1, 2$ according to whether $z < H$ or $z > H$ and x, z are obtained from ξ, η according to eq. (19). From eq. (4) and using the closure condition at crack tips ($\tilde{\alpha}_0 = 0$) the displacement discontinuity is written as

$$\Delta\tilde{u}(z) = \Delta\tilde{u}(\ell\xi + c) = \ell\int_{-1}^{\xi}\tilde{\rho}(\xi')\, d\xi' = -\ell\sqrt{1-\xi^2}\sum_{k=1}^{K}\frac{\tilde{\alpha}_k}{k}U_{k-1}(\xi), \tag{34}$$

where the following result has been employed:

$$\int_{-1}^{\xi}\frac{T_k(\xi')}{\sqrt{1-\xi'^2}}\, d\xi' = \begin{cases} -\dfrac{1}{k}\sqrt{1-\xi^2}\, U_{k-1}(\xi) & \text{if} \quad k > 0 \\ \dfrac{\pi}{2} + \arcsin\xi & \text{if} \quad k = 0. \end{cases}$$

Results for case A

In Fig. 3 the slip $\Delta\tilde{u}$ and the dislocation density distribution $\tilde{\rho}$ are plotted for different values of rigidity ratio $m = \mu_2/\mu_1$, for a crack extending between 3 and 13 km depth; the rigidity of the lower medium is $\mu_2 = 22.5$ GPa, the stress drop is $\Delta\sigma = 5$ MPa and the layer thickness is $H = 2$ km. An order of truncation $K = 20$ and $N = 10$ were chosen as all the numerical results were found to be insensitive to any further increase of these values. It is clear from these plots that even large variations in the rigidity contrast involve only minor changes in $\Delta\tilde{u}$, which increases when decreasing μ_1 (while keeping μ_2 fixed) as the softer layer opposes less resistance to the deformation. Larger changes in $\Delta\tilde{u}$ are obtained if the crack is closer and closer to the interface.

In Fig. 4 the shear stress $\tilde{\sigma}_{xy}$ induced by a crack in a layered half-space with $\mu_2 = 22.5$ GPa and $\mu_1 = 0.1\mu_2$ is plotted and compared with the solution for a homogeneous half-space with uniform rigidity μ_2. The ratio $\mu_2/\mu_1 = 10$ is clearly an extremely high value, but it is chosen here to emphasize the role of layering. Discontinuity of $\tilde{\sigma}_{xy}$ across the interface $z = H$ can be noted. Major differences between the heterogeneous and the homogeneous models are present along the interface, particularly in the proximity of and above the upper tip of

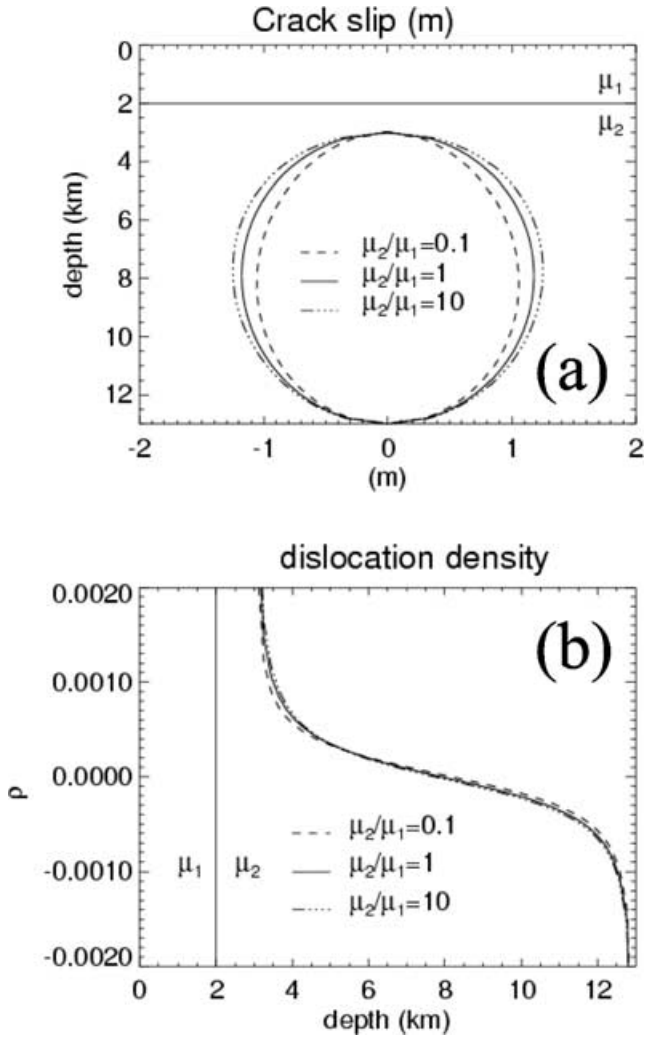

Figure 3. Crack slip and dislocation density distribution in case A, for different values of $m = \mu_2/\mu_1$; $H = 2$ km, $c = 8$ km, $\ell = 5$ km, $\mu_2 = 22.5$ GPa and $\Delta\sigma = 5$ MPa.

the crack ($z = 3$ km): in the lower half-space these differences reach a maximum just below the interface, where the heterogeneous model provides values higher than 3 MPa with respect to the homogeneous model (but note that the stress is unbounded at the crack tip); in the upper layer, the heterogeneous model provides stress values that are lower than those of the homogeneous model with rigidity, $\mu_2 = 22.5$ GPa, but much higher than would be provided by a homogeneous half-space model with rigidity $\mu_1 = 2.25$ GPa (not shown). This is a result of the larger strain concentration present in the heterogeneous model in proximity of the strike direction.

In Fig. 5 the stress component $\tilde{\sigma}_{yz}$ is plotted for $m = 10$ and 1. This component must be continuous across the interface. Consequently, even in the lower half-space, this stress component is lower in the heterogeneous model than in the homogeneous model, since it 'feels' the presence of the softer medium above the interface; a slight increase of stress intensity, with respect to the homogeneous solution, is induced at greater depth (e.g. at 8 km depth), but contour lines do not change appreciably there. The present results are computed for a constant stress drop and accordingly differ somewhat from those shown by Rybicki (1971, 1973), who employed a uniform slip over the fault plane; however, his major finding—that larger stress values are induced by faulting near the interface—is confirmed in crack models as well.

CASE B: CRACK TOUCHING THE INTERFACE

Now consider the case of a crack embedded in the lower half-space and with an upper tip that touches the interface $z = H$ between the two media. Employing the non-dimensional coordinates (19), the equilibrium equation is still given by eq. (17) but, in this case, $c - H = \ell$ (see Fig. 2) and the first term in eq. (18) for $\mathcal{R}_2^{\mathrm{II}}(\xi', \xi)$ is singular in $\xi = \xi' = -1$ because $\lambda - h = 1$. This singularity in the integral kernel adds to the Cauchy singularity $1/(\xi' - \xi)$ in eq. (17). The integral equation (17) is then a generalized Cauchy equation (e.g. Muskhelishvili 1953). Following an asymptotic method developed by Erdogan *et al.* (1973) the singular behaviour, near crack tips $\xi = \pm 1$, of the dislocation density distribution can be studied. We shall not dwell on details, since results pertinent to case B can be obtained from case C, to be discussed next. From the asymptotic study we obtain the following dislocation density distribution:

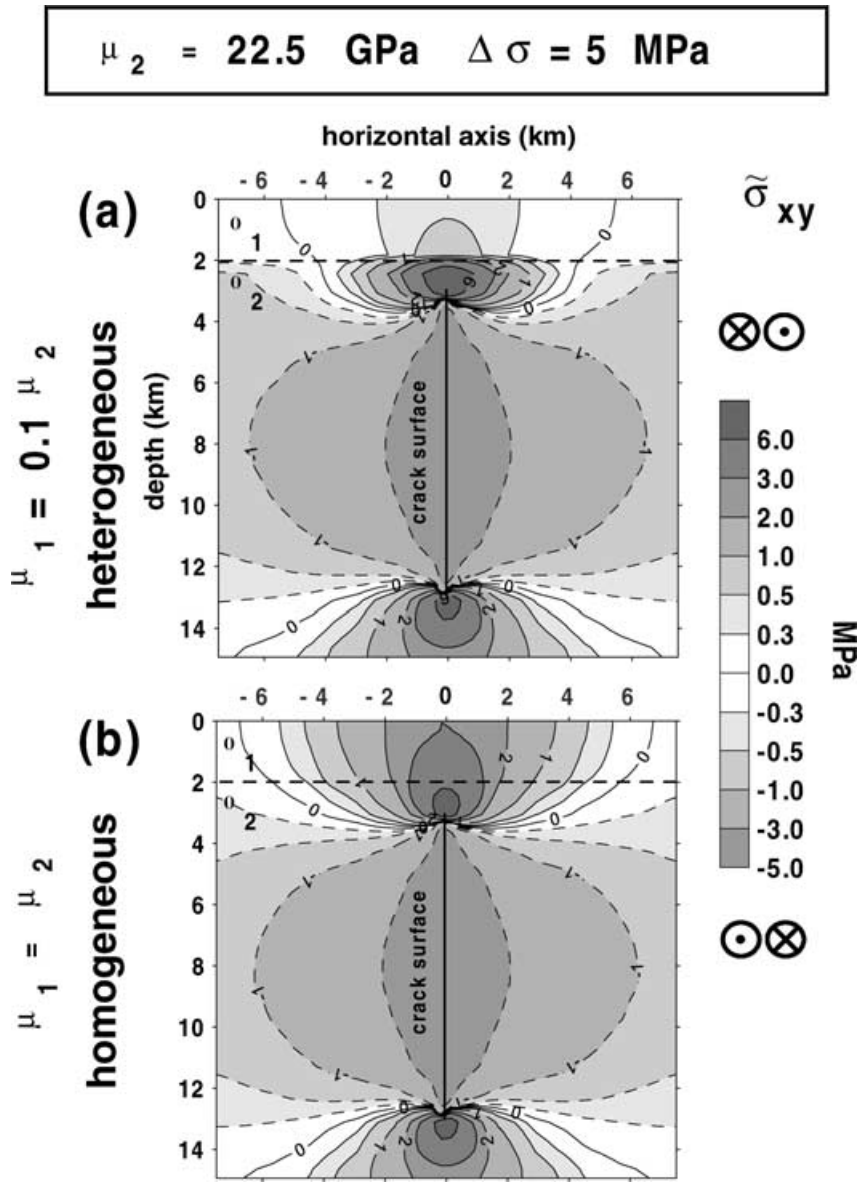

Figure 4. Stress component $\tilde{\sigma}^{c}_{xy}$ induced by crack slip in the heterogeneous medium with $m = 10$ (a) and in the homogeneous medium with $m = 1$ (b). H, c, ℓ, μ_2 and $\Delta\sigma$ as in Fig. 3. Negative values are contoured by dashed lines, positive values by solid lines.

$$\rho(\xi') = R(\xi')\,(1-\xi')^{-1/2}(1+\xi')^{b}, \tag{35}$$

where the exponent b is subject to the constraint $(-1 < b \leq 0)$ (Muskhelishvili 1953) and must fulfil the following condition in order for the left-hand side of eq. (17) (i.e. $\Delta\sigma$) be bounded:

$$b = -\frac{1}{\pi}\arccos\Gamma, \quad \text{with} \quad \Gamma = \frac{\mu_1 - \mu_2}{\mu_1 + \mu_2} \tag{36}$$

and $R(\xi')$ is a regular function with $R(\pm 1) \neq 0$. In Appendix B the exact derivation of this equation can be found as a particular case. Table 1 shows the values of b for different values of $m = \mu_2/\mu_1$. The exponent b is $-1/2$ for the homogeneous case, as expected, and is lower or greater then $-1/2$ according to whether $m > 1$ or $m < 1$; moreover the exponent b tends to approach the value -1 while increasing m.

Proceeding in analogy with case A, we might expand the regular factor $R(\xi')$ in eq. (35) through Jacobi polynomials $P_n^{(-1/2,b)}(\xi')$, which are the orthogonal polynomials for the weight function $w(\xi') = (1-\xi')^{-1/2}(1+\xi')^{b}$. This procedure is described by Erdogan *et al.* (1973), but no convenient analytical expression (such as eq. 22 for case A) can be found, in general, for the singular integrals appearing in eq. (17), so that resort must be made to numerical methods from the beginning. This method of solution for antiplane shear cracks in a layered medium was employed by Morelli *et al.* (1987). However, the same method employed for case A can be employed even in case B, provided that stress values are computed away from the upper crack tip (at $z = H$, i.e. at $\xi = -1$), where the stress is in any case unbounded. Eq. (35) can be rewritten as

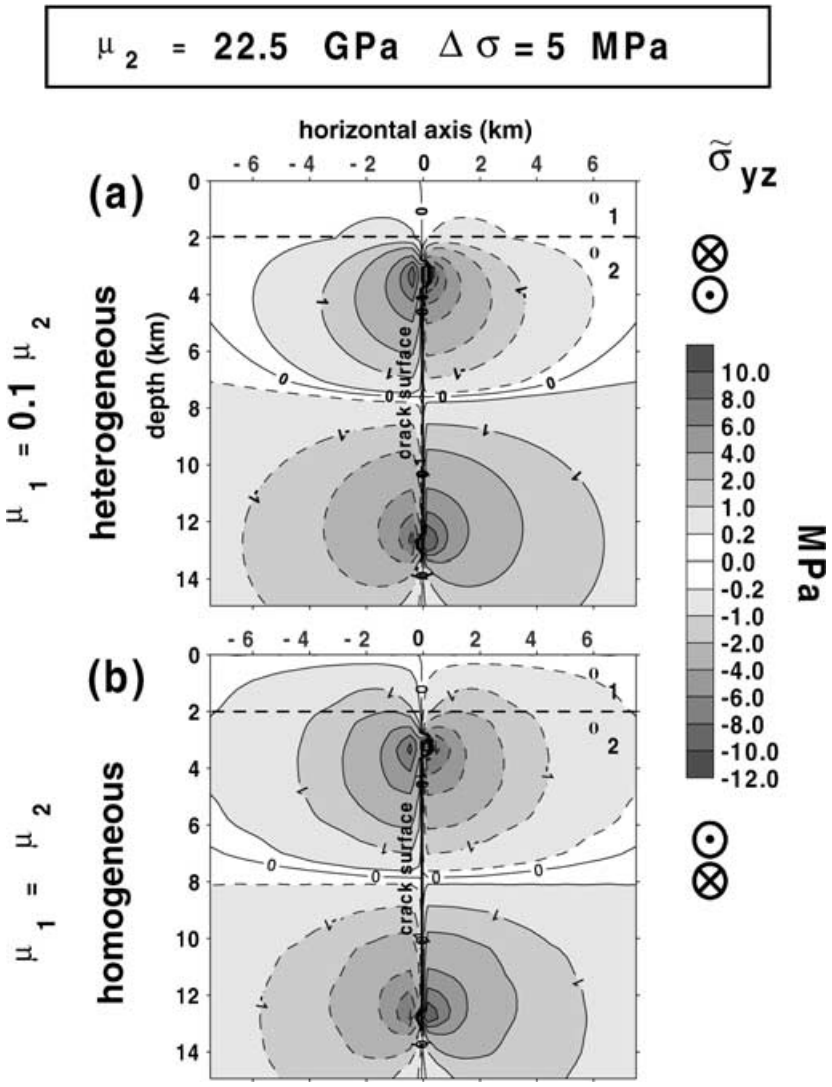

Figure 5. Same as in Fig. 4, for the stress component $\tilde{\sigma}^{c}_{yz}$.

$$\rho(\xi') = \frac{1}{\sqrt{1-\xi'^2}}\left[R(\xi')(1+\xi')^{\frac{1}{2}+b}\right], \tag{37}$$

where

$$\begin{cases} \frac{1}{2}+b>0 & \text{if} \quad m<1 \\ \frac{1}{2}+b=0 & \text{if} \quad m=1 \\ -\frac{1}{2}<\frac{1}{2}+b<0 & \text{if} \quad m>1. \end{cases}$$

From this scheme it is clear that if $m \leq 1$ the factor within square brackets $R(\xi')(1+\xi')^{\frac{1}{2}+b}$ is regular and can be expanded in a uniformly convergent expansion of Chebyshev polynomials; if $m > 1$, otherwise, it has a square-integrable singularity and, consequently, the expansion in Chebyshev polynomials will be convergent only in the mean.

With the above-mentioned caveat, $\rho(\xi')$ can be written, as in case A, in the following way:

$$\rho(\xi') = \frac{1}{\sqrt{1-\xi'^2}} \sum_{k=0}^{\infty} \alpha_k T_k(\xi') \tag{38}$$

Table 1. Singularity order for case B.

m	*b*
0.1	−0.195
0.25	−0.295
0.5	−0.392
1	−0.5
2	−0.608
4	−0.705
10	−0.805

with

$$\sum_{k=0}^{\infty} \alpha_k T_k(\xi') = R(\xi')(1+\xi')^{\frac{1}{2}+b}.$$

In order to solve the problem, a truncation $\tilde{\rho}$ of the previous series is taken (order of truncation K). Then, we can follow the same technique of solution described for case A, with the only difference being that the integral with respect to ξ' in I_1 in eq. (25) contains a singular term in case B, but the singularity can be disposed of analytically (see Appendix A).

From physical intuition, we would expect that case B should be obtained as the limit of case A when the crack tip in $c-\ell$ approaches H. Actually, as far as $c-\ell > H$ the regular factor $R(\xi')$ in eq. (20) is bounded and non-vanishing at $\xi' = -1$ but, when $c-\ell$ approaches H, $R(-1)$ increases indefinitely if $m > 1$ and becomes vanishingly small if $m < 1$. This helps us understand why the singularity of ρ in case B differs from case A. The best we can hope when $c-\ell$ approaches H is that $\tilde{\rho}$ of case A approaches $\tilde{\rho}$ of case B in the mean, since the two densities have different singularities. Accordingly the question is: how much does this approximation affect the computation of observable quantities? It is easily shown that convergence in the mean of $\tilde{\rho}(\xi')$ allows one to obtain pointwise convergence of all observable quantities (slip, displacement and stress fields), which are computed from square-integrable elementary expressions, weighted with $\tilde{\rho}$. This is not the case only for the stress components at the crack tips (where the stress is in any case unbounded). This statement can be proved in the following way: if $\tilde{O}_K(\xi)$ is an observable computed from the truncated solution to Kth order:

$$\tilde{O}_K(\xi) = \int_{-1}^{1} \tilde{\rho}_K(\xi') f(\xi', \xi)\, d\xi'$$

where $f(\xi', \xi)$ is a square-integrable function of ξ' over the interval $(-1, 1)$, the deviation between the estimated and the 'true' values is (employing the Cauchy–Schwarz inequality)

$$|\tilde{O}_K(\xi) - O(\xi)|^2 = \left| \int_{-1}^{1} \{\tilde{\rho}_K(\xi') - \rho(\xi')\} f(\xi', \xi)\, d\xi' \right|^2 \leq \int_{-1}^{1} |f(\xi', \xi)|^2\, d\xi' \int_{-1}^{1} |\tilde{\rho}_K(\xi') - \rho(\xi')|^2\, d\xi'$$

showing that convergence in the mean of $\tilde{\rho}_K$ to ρ provides pointwise convergence of $\tilde{O}_K$ to O. Further considerations on the convergence of the present and other methods of estimating $O(\xi)$ in dislocation problems (such as the boundary element method) can be found in Bonafede & Rivalta (1999a).

Results for case B

In Fig. 6, $\Delta\tilde{u}(\xi)$ and $\tilde{\rho}(\xi')$ are plotted for a shear crack extending between 2 and 12 km in depth, with $\Delta\sigma = 5$ MPa and $H = 2$ km. Several values of m have been considered; Fig. 6(a) shows the crack slip for different values of m. As in case A, crack slip increases for decreasing μ_1; furthermore, a remarkable asymmetry with respect to depth can be appreciated in the crack shape for $m \neq 1$ and especially for $m > 1$ as, in this case, the close proximity to the soft layer greatly enhances the asymmetry, which would be present even for a homogeneous medium owing to the proximity to the free surface. The maximum value of the slip is in any case shifted from the crack midpoint depth (elliptic crack in a homogeneous space) towards the softer medium.

Fig. 6(b) shows $\tilde{\rho}$ for the same crack models; in the case where $m = 10$ an oscillatory behaviour is evident in $\tilde{\rho}$, which is typical for a Fourier expansion of a singular function, which converges slowly. No such oscillations appear when $m \leq 1$, since in this case the function to be expanded (the term within square brackets in eq. 37) is regular. No oscillations are present in $\Delta\tilde{u}$ (Fig. 6a), even when $m = 10$, since the slip function is bounded and continuous (its series expansion converges faster, accordingly).

CASE C: CRACK CROSSING THE INTERFACE

Let us consider a crack extending from $z = H - 2\ell_1$ in the upper layer to $z = H + 2\ell_2$, in half-space 2 (Fig. 2C). It is convenient to split the crack into two interacting sections, each embedded in one medium and both open at the interface $z = H$ where they must join each other. As discussed previously, the dislocation density $\rho(z_0)$ in eq. (2) will be split into two subdomains: a density $\rho_1(z_0)$ in layer 1 ($H - 2\ell_1 < z_0 < H$) and a density $\rho_2(z_0)$ in half-space 2($H < z_0 < H + 2\ell_2$). The mid-points of the two crack sections are, respectively, $c_1 = H - \ell_1$ and $c_2 = H + \ell_2$. In analogy with cases A and B, it is convenient to introduce the following non-dimensional variables:

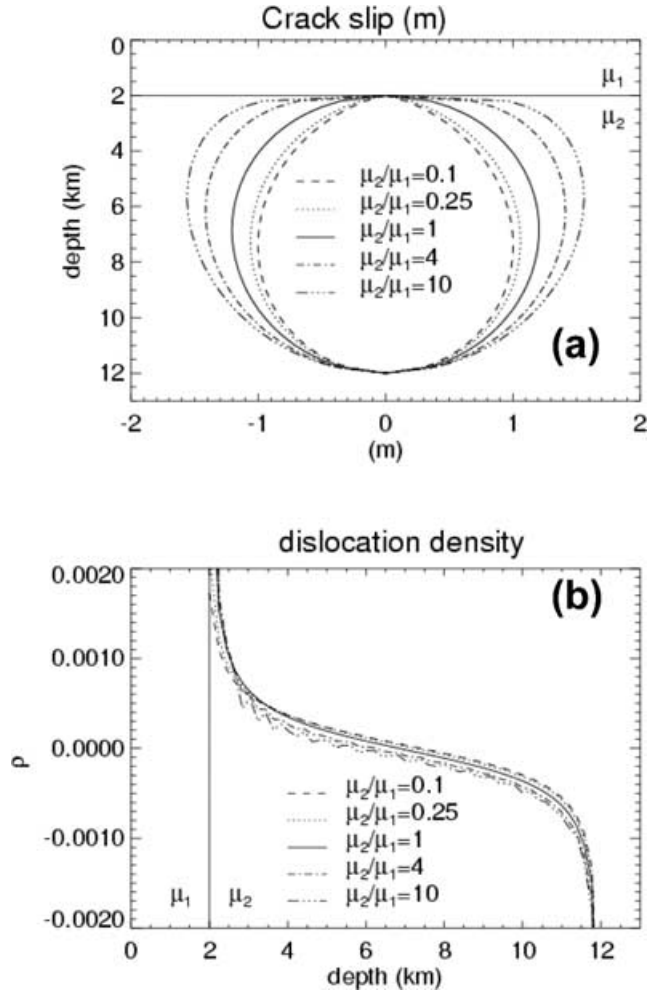

Figure 6. Crack slip (a) in case B for several values of $m = \mu_2/\mu_1$; $H = 2$ km, $c = 7$ km, $\ell = 5$ km, $\mu_2 = 22.5$ GPa and $\Delta\sigma = 5$ MPa. Dislocation density distribution (b) in case B, for several values of m.

$$\xi_1 = (z - c_1)/\ell_1 \quad \text{if} \quad z < H, \quad \xi_1' = (z_0 - c_1)/\ell_1 \quad \text{if} \quad z_0 < H,$$

$$\xi_2 = (z - c_2)/\ell_2 \quad \text{if} \quad z > H, \quad \xi_2' = (z_0 - c_2)/\ell_2 \quad \text{if} \quad z_0 > H,$$

$$\lambda_{11} = c_1/\ell_1, \quad \lambda_{12} = c_1/\ell_2, \tag{39}$$

$$\lambda_{21} = c_2/\ell_1, \quad \lambda_{22} = c_2/\ell_2,$$

$$h_1 = H/\ell_1, \quad h_2 = H/\ell_2.$$

The equilibrium eq. (14) can be written employing eqs (10)–(13). Consequently, we have the following system for the unknown functions ρ_1 and ρ_2 (where singular terms are singled out):

$$\begin{aligned}\frac{2\pi}{\mu_1}\Delta\sigma_1(\xi_1) = {} & \int_{-1}^{1}\frac{\rho_1(\xi_1')\,d\xi_1'}{\xi_1 - \xi_1'} - \Gamma\int_{-1}^{1}\frac{\rho_1(\xi_1')\,d\xi_1'}{\xi_1 + \xi_1' - 2} - \frac{2m}{1+m}\int_{-1}^{1}\frac{\rho_2(\xi_2')\,d\xi_2'}{\xi_2' - \frac{\ell_1}{\ell_2}\xi_1 + 1 + \frac{\ell_1}{\ell_2}} + \int_{-1}^{1}\rho_1(\xi_1')\mathcal{R}_{11}(\xi_1, \xi_1')\,d\xi_1' \\ & + \int_{-1}^{1}\rho_2(\xi_2')\mathcal{R}_{12}(\xi_1, \xi_2')\,d\xi_2' \\ \frac{2\pi}{\mu_2}\Delta\sigma_2(\xi_2) = {} & \int_{-1}^{1}\frac{\rho_2(\xi_2')\,d\xi_2'}{\xi_2 - \xi_2'} + \Gamma\int_{-1}^{1}\frac{\rho_2(\xi_2')\,d\xi_2'}{\xi_2 + \xi_2' + 2} - \frac{2}{1+m}\int_{-1}^{1}\frac{\rho_1(\xi_1')\,d\xi_1'}{\xi_1' - \frac{\ell_2}{\ell_1}\xi_2 - 1 - \frac{\ell_2}{\ell_1}} + \int_{-1}^{1}\rho_1(\xi_1')\mathcal{R}_{21}(\xi_2, \xi_1')\,d\xi_1' \\ & + \int_{-1}^{1}\rho_2(\xi_2')\mathcal{R}_{22}(\xi_2, \xi_2')\,d\xi_2',\end{aligned} \tag{40}$$

where the regular kernels $\mathcal{R}_{ij}$ are

$$\mathcal{R}_{11}(\xi_1,\xi_1') = -\frac{1}{\xi_1+\xi_1'+2\lambda_{11}} + \sum_{n=1}^{\infty}\Gamma^n\left[\frac{1}{\xi_1-\xi_1'+2nh_1}+\frac{1}{\xi_1-\xi_1'-2nh_1}-\frac{1}{\xi_1+\xi_1'+2\lambda_{11}+2nh_1}-\frac{\Gamma}{\xi_1+\xi_1'+2\lambda_{11}-2(n+1)h_1}\right]$$

$$\mathcal{R}_{12}(\xi_1,\xi_2') = -\frac{2m}{1+m}\sum_{n=0}^{\infty}\Gamma^n\left[\frac{1}{\frac{\ell_1}{\ell_2}\xi_1+\xi_2'+\lambda_{12}+\lambda_{22}+2nh_2}-\frac{\Gamma}{\frac{\ell_1}{\ell_2}\xi_1-\xi_2'+\lambda_{12}-\lambda_{22}-2(n+1)h_2}\right]$$

$$\mathcal{R}_{21}(\xi_2,\xi_1') = -\frac{2}{1+m}\sum_{n=0}^{\infty}\Gamma^n\left[\frac{1}{\frac{\ell_2}{\ell_1}\xi_2+\xi_1'+\lambda_{11}+\lambda_{21}+2nh_1}-\frac{\Gamma}{\frac{\ell_2}{\ell_1}\xi_2-\xi_1'+\lambda_{21}-\lambda_{11}+2(n+1)h_1}\right]$$

$$\mathcal{R}_{22}(\xi_2,\xi_2') = -\frac{4m}{(1+m)^2}\sum_{n=0}^{\infty}\Gamma^n\frac{1}{\xi_2+\xi_2'+2(\lambda_{22}+nh_2)}.$$

Apart from Cauchy kernels—the first term in the right-hand side of both eqs (40)—the second and third terms on the right-hand side are also singular for $\xi_1=\xi_1'=1$ and $\xi_2=\xi_2'=-1$, corresponding to $z=z_0=H$. All other terms appearing in the kernels $\mathcal{R}_{ij}$ are regular (Fredholm kernels). It may be mentioned that the presence of the kernels $\mathcal{R}_{ij}$ written above are strictly related to the presence of the free surface: this is clearly seen if we let $H\to\infty$ while keeping ℓ_1 and ℓ_2 finite, since $c_1, c_2, h_1, h_2, \lambda_{ij}\to\infty$. The case of two welded half-spaces is then simply obtained by letting $\mathcal{R}_{ij}=0$ in eq. (40).

Thus the system (40) is formed by two coupled equations of generalized Cauchy type. As for case B, the first problem to be solved is determining the order of singularity of $\rho_1(\xi_1')$ near $\xi_1'=1$ and of $\rho_2(\xi_2')$ near $\xi_2'=-1$. Since, furthermore, both crack sections are open at the interface, we must state two additional constraints (to replace the closure condition employed in cases A and B) in order that the problem may yield a unique solution.

Supplementary conditions

The first supplementary condition necessary to make the present problem well-posed is easily derived from the continuity condition of crack slip at the interface between the two media. From equations similar to eq. (4), imposing the closure conditions at $z=H-2\ell_1$ for ρ_1 and at $z=H+2\ell_2$ for ρ_2, the slip continuity condition at $z=H$ yields

$$\Delta u_1(\xi_1=1)=\Delta u_2(\xi_2=-1)\Rightarrow \ell_1\int_{-1}^{1}\rho_1(\xi_1')\,d\xi_1' = -\ell_2\int_{-1}^{1}\rho_2(\xi_2')\,d\xi_2'. \tag{41}$$

Another condition is needed to provide bounded stress drop values over the crack plane near $z=H$. This can be obtained from an asymptotic study that determines the types of singularities present in the dislocation density at crack tips. Here the main results are given; full details can be found in Appendix B.

Introduce for ρ_1 and ρ_2 expressions analogous to eq. (20):

$$\begin{aligned}\rho_1(\xi_1) &= (1-\xi_1)^{a_1}(1+\xi_1)^{b_1}R_1(\xi_1)\\ \rho_2(\xi_2) &= (1-\xi_2)^{a_2}(1+\xi_2)^{b_2}R_2(\xi_2),\end{aligned} \tag{42}$$

where all the exponents must obey $-1<a_1,b_1,a_2,b_2\le 0$ and $R_1(\pm1)\neq 0$, $R_2(\pm1)\neq 0$. Introducing these expressions in eq. (40) the right-hand side of both equilibrium equations would provide unbounded values at $\xi_1=-1^+$ and $\xi_2=1^-$ unless $b_1=-1/2$ and $a_2=-1/2$ (as expected since each of these crack tips is embedded within a locally homogeneous medium); unbounded values would also be present at interface crack tips $\xi_1=1^-$ and $\xi_2=-1^+$ unless $a_1=b_2=\omega$, in which case unbounded terms near the interface may cancel. Non-trivial solutions for $R_1(1)$ and $R_2(-1)$ are obtained if ω obeys the following equation, under the constraint $-1<\omega\le 0$:

$$\cos^2\pi\omega-1=0\Rightarrow\omega=0 \tag{43}$$

(see Appendix B) and in such a case the following relation must hold:

$$\frac{R_1(1)}{R_2(-1)}=\frac{\rho_1(z_0=H^-)}{\rho_2(z_0=H^+)}=m. \tag{44}$$

This is the second necessary condition to be satisfied by the dislocation densities. Eq. (44) shows that the overall distribution ρ has a jump discontinuity at the interface (unless $m=1$, in which case the medium is homogeneous). An interesting result is that the ratio $R_1(1)/R_2(-1)$ does not depend on the crack geometry (i.e. ℓ_1,ℓ_2), nor on the stress drop $\Delta\sigma$ (even if it were highly variable over the crack plane), but it depends only on the rigidity ratio m.

The present results also apply to any interface in a multilayered medium, since no singularity at the interface between two layers may arise from kernels accounting for the presence of dislocations in more distant layers.

It may be mentioned that the condition (44) reflects the fact that continuity of tractions along the interface must be obtained even in the limit $x \to 0^{\pm}$:

$$\lim_{x\to 0^+} \lim_{z\to H^-} \mu_1 \left(\frac{\partial u_1}{\partial z}\right) = \lim_{x\to 0^+} \lim_{z\to H^+} \mu_2 \left(\frac{\partial u_2}{\partial z}\right).$$

If the order in which limits and derivatives are taken could be exchanged, we should obtain immediately eq. (44), employing the definitions

$$\lim_{x\to 0^+} u_i = \frac{1}{2}\Delta u \quad \text{and} \quad \rho_i = \frac{\partial \Delta u_i}{\partial z} \qquad i = 1, 2.$$

However, the possibility of exchanging the order of limits is generally not allowed at singular points such as crack tips (for instance, bounded and unbounded stress values are generally obtained while approaching a crack tip moving over or out of the crack plane, respectively). The previous asymptotic study shows that exchanging the order of limits may be allowed at interface crack tips. It must also be mentioned that the previous results are restricted to antiplane shear cracks (mode III): a similar study (Bonafede & Rivalta 1999a) for tensile cracks (mode I), opening across the interface between two media, shows that the dislocation density distribution presents unbounded singularities on both sides of the interface, and the ratio $R_1(1)/R_2(-1)$ appearing in expansions similar to eq. (42) is dependent on the lengths of the crack sections.

Method of solution

The asymptotic study in the previous section shows that finite stress release is obtained over both crack sections if the exponents appearing in eq. (42) are $b_1 = a_2 = -\frac{1}{2}$ and $a_1 = b_2 = 0$, with $\frac{R_1(1)}{R_2(-1)} = \frac{\mu_2}{\mu_1}$.

The form of the singular factors in eq. (42) suggests expanding $R(\xi)$ in Jacobi polynomials $P_n^{(a,b)}(\xi)$, which are orthogonal if the weight function $w(\xi) = (1-\xi)^a(1+\xi)^b$ is employed (see e.g. Abramowitz & Stegun 1964). Let us consider the dislocation density $\rho_2(\xi_2)$. Taking into account the conditions $a_2 = -\frac{1}{2}$ and $b_2 = 0$ we may write

$$\rho_2(\xi_2) = \frac{1}{\sqrt{1-\xi_2}} \sum_{k=0}^{\infty} c_k P_k^{(-1/2,0)}(\xi_2), \quad -1 < \xi_2 < 1. \tag{45}$$

Interrelations among orthogonal polynomials allow us to write

$$P_k^{(-1/2,0)}(\xi_2) = (-1)^k P_k^{(0,-1/2)}(-\xi_2) = (-1)^k C_{2k}^{(1/2)}(t_2) = (-1)^k P_{2k}(t_2), \quad \text{with} \quad t_2 = \sqrt{\frac{1-\xi_2}{2}}, \tag{46}$$

where $C_k^{(\alpha)}(t)$ are ultraspherical (Gegenbauer) polynomials that, if $\alpha = \frac{1}{2}$, reproduce Legendre polynomials $P_k(t)$. The normalized dislocation density $\rho_2(\xi_2)$ can then be written as

$$\rho_2(\xi_2) = \frac{1}{t_2} \sum_{k=0}^{\infty} \alpha_k P_{2k}(t_2), \quad -1 < \xi_2 < 1, \quad 0 < t_2 < 1, \tag{47}$$

where α_k coefficients differ from c_k in eq. (45) by a factor of $(-1)^k/\sqrt{2}$. The presence of the singular factor t_2^{-1} in eq. (47) should be of no concern, since ρ_2 always appears through integrals when observable quantities are considered and $d\xi_2 = -4t_2\, dt_2$. For instance, the displacement discontinuity Δu_2 may be obtained as

$$\Delta u_2(\xi_2) = \ell_2 \int_{-1}^{\xi_2} \rho_2(\xi)\, d\xi + C = 4\ell_2 \int_{t_2}^{1} \sum_k \alpha_k P_{2k}(t)\, dt + C = -4\ell_2 \int_0^{t_2} \sum_k \alpha_k P_{2k}(t)\, dt, \tag{48}$$

where, in the last equality, the closure condition $\Delta u_2(\xi_2 = 1) = 0$ has been employed to fix the integration constant C. The slip amplitude at the interface $\xi_2 = -1$ (i.e. at $t_2 = 1$) can be easily computed from eq. (48), employing the property that $P_{2k}(t)$ polynomials are even functions and are orthogonal over $(-1, 1)$ to $P_0(t) = 1$ if $k \neq 0$:

$$\Delta u_2(\xi_2 = -1) = -4\ell_2 \int_0^1 \sum_k \alpha_k P_{2k}(t_2)\, dt_2 = -2\ell_2 \sum_k \alpha_k \int_{-1}^1 P_{2k}(t)\, dt = -4\ell_2\alpha_0. \tag{49}$$

Employing the same method, the normalized dislocation density $\rho_1(\xi_1)$ can be written through an expansion similar to eq. (47):

$$\rho_1(\xi_1) = \frac{1}{t_1} \sum_{k=0}^{\infty} \beta_k P_{2k}(t_1), \quad t_1 = \sqrt{\frac{1+\xi_1}{2}}, \quad -1 < \xi_1 < 1, \quad 0 < t_1 < 1 \tag{50}$$

and the crack slip at the interface (i.e. in $\xi_1 = 1$) is

$$\Delta u_1(\xi_1 = 1) = 4\ell_1\beta_0. \tag{51}$$

Since we assume that the interface is a welded boundary, the first supplementary condition (41) is simply

$$\beta_0 = -\frac{\ell_2}{\ell_1}\alpha_0. \tag{52}$$

A further link between β_k and α_k coefficients is imposed by the second supplementary condition (44). Since $P_{2k}(1) = 1$, from eqs (47) and (50) we obtain simply

$$\sum_{k=0}^{\infty}\beta_k = \frac{\mu_2}{\mu_1}\sum_{k=0}^{\infty}\alpha_k. \tag{53}$$

The equilibrium equation (40) provides further relationships among the α_k and β_k coefficients appearing in eqs (47) and (50). If these expressions for ρ_1 and ρ_2 are inserted into eq. (40) the following singular integrals must be evaluated in the principal-value sense:

$$\begin{aligned}
&I_{11}(\xi_1) = \int_{-1}^{1}\frac{\rho_1(\xi_1')\,d\xi_1'}{\xi_1-\xi_1'}, \quad I_{12}(\xi_1) = \int_{-1}^{1}\frac{\rho_1(\xi_1')\,d\xi_1'}{\xi_1+\xi_1'-2}, \quad I_{13}(\xi_1) = \int_{-1}^{1}\frac{\rho_2(\xi_2')\,d\xi_2'}{\xi_2'+1+\frac{\ell_1}{\ell_2}(1-\xi_1)},\\
&I_{21}(\xi_2) = \int_{-1}^{1}\frac{\rho_2(\xi_2')\,d\xi_2'}{\xi_2-\xi_2'}, \quad I_{22}(\xi_2) = \int_{-1}^{1}\frac{\rho_2(\xi_2')\,d\xi_2'}{\xi_2+\xi_2'+2}, \quad I_{23}(\xi_2) = \int_{-1}^{1}\frac{\rho_1(\xi_1')\,d\xi_1'}{\xi_1'-1-\frac{\ell_2}{\ell_1}(1+\xi_2)}.
\end{aligned} \tag{54}$$

These can be evaluated analytically, exploiting the even property of P_{2k} polynomials, and the integral formula (e.g. Gradshteyn & Ryzhik 1965)

$$\int_{-1}^{1}\frac{P_k(t')}{t-t'}\,dt' = 2Q_k(t),$$

where $Q_k(t)$ are Legendre functions of the second kind, which possess a logarithmic singularity at $t = \pm 1$ (this type of singularity is expected from the asymptotic study considered in Appendix B). Computational details are given in Appendix C. We obtain

$$\begin{aligned}
I_{11} &= \frac{2}{t_1}\sum_{k=0}^{\infty}\beta_k Q_{2k}(t_1), && t_1 = \sqrt{\frac{1+\xi_1}{2}}, && t_1 \in (0,1)\\
I_{12} &= -\frac{2}{u_1}\sum_{k=0}^{\infty}\beta_k Q_{2k}(u_1), && u_1 = \sqrt{\frac{3-\xi_1}{2}}, && u_1 \in (1,\sqrt{2})\\
I_{13} &= \frac{2}{v_1}\sum_{k=0}^{\infty}\alpha_k Q_{2k}(v_1), && v_1 = \sqrt{1+\frac{\ell_1}{\ell_2}\frac{1-\xi_1}{2}}, && v_1 \in \left(1,\sqrt{1+\frac{\ell_1}{\ell_2}}\right)\\
I_{21} &= -\frac{2}{t_2}\sum_{k=0}^{\infty}\alpha_k Q_{2k}(t_2), && t_2 = \sqrt{\frac{1-\xi_2}{2}}, && t_2 \in (0,1)\\
I_{22} &= +\frac{2}{u_2}\sum_{k=0}^{\infty}\alpha_k Q_{2k}(u_2), && u_2 = \sqrt{\frac{3+\xi_2}{2}}, && u_2 \in (1,\sqrt{2})\\
I_{23} &= -\frac{2}{v_2}\sum_{k=0}^{\infty}\beta_k Q_{2k}(v_2), && v_2 = \sqrt{1+\frac{\ell_2}{\ell_1}\frac{1+\xi_2}{2}}, && v_2 \in \left(1,\sqrt{1+\frac{\ell_2}{\ell_1}}\right).
\end{aligned} \tag{55}$$

These integrals are all that is needed to solve the simpler problem of two welded half-spaces, since the regular kernels $\mathcal{R}_{ij}$ in eq. (40) vanish if $H = \infty$.

The presence of the free surface when H is finite, complicates the problem in two ways. First, the sum over mirror dislocations (the sum over the index n appearing in $\mathcal{R}_{ij}$) must be truncated—for computational purposes—to a suitable finite order N; truncation can be performed in such a way as to match the free-surface condition exactly, or to match the welded boundary condition exactly, but only when $N \to \infty$ can both conditions be matched simultaneously. Second, the integrals containing the regular kernels $\mathcal{R}_{ij}$ in eq. (40) must be evaluated: these can be evaluated analytically, as described in Appendix C.

The two conditions (52) and (53) cannot be satisfied if only the first term ($k = 0$) is considered in the expansions (47) and (50). The minimum order of truncation to be employed in these expansions, is then $K \geq 1$. It will be shown that $K = 2$ already provides very accurate results.

The stress drop discontinuity

In order to avoid inessential complications, let us restrict ourselves momentarily to considering the problem of two welded elastic half-spaces (in which case kernels $\mathcal{R}_{ij}$ in eq. 40 vanish). In eq. (55) $t_1, u_1, v_1 \to 1$ when $\xi_1 \to 1$, $t_2, u_2, v_2 \to 1$ when $\xi_2 \to -1$, and

$$Q_k(1 \pm \epsilon) = \frac{1}{2} \ln \frac{2}{\epsilon} - \sum_{j=1}^{k} \frac{1}{j} + o(\epsilon)$$

when $\epsilon \to 0^+$ (from the explicit expression of Q_k in terms of P_k, given, for example, in Gradshteyn & Ryzhik 1965, eq. 8.831—reproduced in eq. C5 of Appendix C); from these limiting values, it may be easily checked that

$$I_{11} - \Gamma I_{12} - \frac{2m}{1+m} I_{13} \to \frac{2m}{1+m} \ln \frac{\ell_1}{\ell_2} \sum_k \alpha_k \quad \text{when} \quad \xi_1 \to 1 \tag{56}$$

and $I_{21} + \Gamma I_{22} - \frac{2}{1+m} I_{23}$ tends to the same finite limit when $\xi_2 \to -1$ provided that eq. (53) holds. That these limits are finite is a necessary condition for the two eqs (40) to be valid, since $\Delta\sigma$ is assumed to be bounded. However, the equality of these two limits entails that

$$\lim_{\xi_1 \to 1^+} \frac{\Delta\sigma_1(\xi_1)}{\mu_1} = \lim_{\xi_2 \to -1^-} \frac{\Delta\sigma_2(\xi_2)}{\mu_2} \tag{57}$$

showing that the stress drop cannot be assigned arbitrarily over each crack section, if the non-singularity condition (53) is to be fulfilled. This condition has been shown to be related to the welded boundary condition, which must be imposed over the interface (see the argument following eq. 44).

The constraint (57) can be shown to be a necessary corollary of the welded boundary conditions, in the following way: since the only non-vanishing component of the displacement field is $u_y(x, z)$, values of the stress component σ_{xy} induced by crack slip along both sides of the interface are, respectively,

$$\sigma_{xy}(x, z = H^-) = \mu_1 \frac{\partial u_y}{\partial x} \quad \text{and} \quad \sigma_{xy}(x, z = H^+) = \mu_2 \frac{\partial u_y}{\partial x}. \tag{58}$$

When $x \to 0$, these must reproduce (apart from a difference in sign) the stress drop values $\Delta\sigma_1$ in $z = H^-$ and $\Delta\sigma_2$ in $z = H^+$. Now, the welded boundary condition $u_y(x, z = H^-) = u_y(x, z = H^+)$ requires that

$$\left(\frac{\partial u_y}{\partial x} \right)_{z=H^-} = \left(\frac{\partial u_y}{\partial x} \right)_{z=H^+} \tag{59}$$

and this, in the limit when $x \to 0$, requires that the two stress drop values eq. (58) across the interface must be proportional to the local rigidity values (we have shown in the previous section that exchanging the orders in which the two limits $z \to H^{\pm}$ and $x \to 0$ are taken is allowed at the interface crack tips).

In conclusion, three constraints are found for the crack problem in case C: eq. (52) requires that the interface is welded even in the proximity of the crack plane, eq. (53) accounts for displacement continuity and for finite stress drop values at the interface, but it also imposes, through eq. (57), that the stress drop $\Delta\sigma$ must have a jump discontinuity at the interface, related to the rigidity jump.

It may be mentioned that no similar condition apply to mode-I (tensile) and mode-II (dip-slip) crack models (e.g. Bonafede & Rivalta 1999b, Rivalta *et al.* 2002), for two reasons: first, two displacement components are non-vanishing in mode-I and mode-II crack models so that no discontinuity of a stress component follows from the continuity of displacements across the interface; second, the different geometrical relationships between the interface plane and the released traction require that the stress drop may be assigned arbitrarily in mode-I cracks (the σ_{xx} component need not be continuous across the interface), while it must be continuous in mode-II cracks (the σ_{xz} component must be continuous, being equal to the component σ_{zx} applied over the interface).

Results for case C

In Fig. 7 the slip function Δu and the stress drop $\Delta\sigma$ are shown, as computed from the truncation of eqs (50) and (47) to $k \leq 2$. The free surface is ignored ($H = \infty$). A stepwise constant stress drop profile with $\Delta\sigma_1 = 1$ MPa, $\Delta\sigma_2 = 3$ MPa is employed, for two welded half-spaces with $\mu_1 = 10$ GPa, $\mu_2 = 30$ GPa. A kink in the slip function at the interface crossing is associated with the discontinuity in the dislocation density. Such a kink is concave if the crack has a larger extension in the softer medium, convex if the crack has a larger extension in the harder medium; if the crack has equal extensions in both media, the kink disappears and the slip function is surprisingly similar to the classical elliptical shape that would be typical of a homogeneous medium. The accuracy of the solution can be checked by comparison of the left- and right-hand sides of eq. (40): it appears that the stress drop is reproduced with uniform accuracy to better than 95 per cent by employing only three terms in each of the expansions for ρ_1 and ρ_2 (Fig. 7b). Since the elementary solutions for the displacement field equation (8) and the elementary solutions for the stress components eq. (9) satisfy the equilibrium equation and the boundary conditions (free surface in $z = 0$ and welded interface at $z = H$), any linear superposition of elementary solutions will also satisfy the same equation and conditions: accordingly, the approximate crack solutions obtained from truncated expansions of eqs (50) and (47) are exact solutions all over the layered medium for the approximate stress drop computed as the right-hand side of eq. (40). Employing four terms in the expansions (50) and (47), the accuracy of the solution increases to above 99 per cent.

Fig. 8 shows the non-vanishing stress components induced by a shear crack extending from 5 to 20 km depth. Here, the free surface is accounted for, as can be seen from the vanishing values of σ_{yz} in $z = 0$. A welded interface at 15 km, separates a lower crust with rigidity

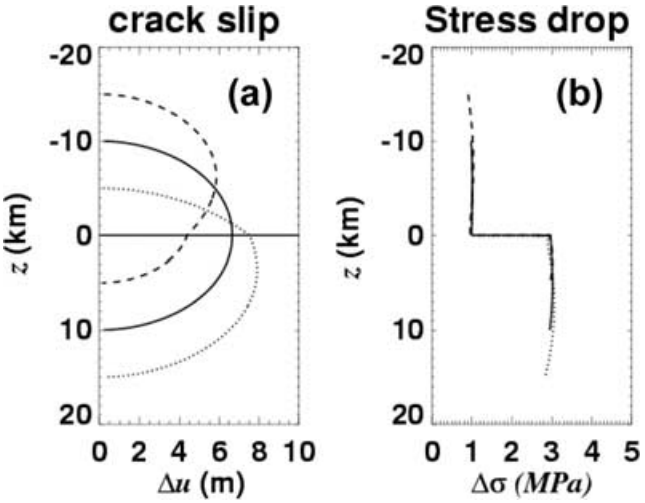

Figure 7. (a) Crack slip in case C: the interface is at $z = 0$ and the free surface is ignored ($H = \infty$). Rigidity values $\mu_1 = 10$ GPa, $\mu_2 = 30$ GPa; the stress drop discontinuity condition is assumed to hold, with $\Delta\sigma_1 = 1$ MPa, and $\Delta\sigma_2 = 3$ MPa. The expansions for the dislocation densities ρ_1 and ρ_2 are truncated to $k \leq 2$. (b) The stress drop approximation obtained from the right-hand side of eq. (40) truncated to $k \leq 2$.

$\mu_2 = 44.1$ GPa from an upper layer with $\mu_1 = \frac{1}{1.7}\mu_2$, pertinent to the transition between the upper crust and the lower crust according to the PREM model. The stress drop is assumed to be $\Delta\sigma_2 = 1.7$ MPa and $\Delta\sigma_1 = 1$ MPa, respectively, in the two media, complying with the stress drop discontinuity condition. The stress components obtained for the layered medium are compared with a homogeneous medium with uniform rigidity and uniform stress drop μ_1 and $\Delta\sigma_1$. Of course, the main difference between the two cases is found in the higher stress appearing in the harder medium for the inhomogeneous model. This is a result of the higher stress drop $\Delta\sigma_2$ in medium 2. Thus, most of the difference between the stress components in the heterogeneous and the homogeneous models seems to be related to the different rigidity more than to a difference in strain. In order to appreciate this point in greater detail, the strain components of the homogeneous model are subtracted from those of the heterogeneous model in panels (e) and (f): strain differences were normalized to $\Delta\sigma/\mu$ (the uniform strain value over the fault plane). Apart from the strain concentration near crack tips, two lobes of positive strain $\epsilon_{xy} = \frac{1}{2}\frac{\partial u_y}{\partial x}$ appear along the interface in (e). The boundary condition of stress continuity across the interface makes the strain difference of the component ϵ_{yz} much larger in medium 2 (Fig. 8f).

Figs 7(a) and 8(e) show that, owing to the stress-drop discontinuity condition, the layered model provides results very similar to the homogeneous model as far as the strain (not the stress) is concerned. This is best shown by Fig. 9, where the surface displacement u_y is plotted versus the distance x from the fault. Here a crack is considered that penetrates across a discontinuity at 5 km depth separating a sedimentary rock with $\mu_1 = 10$ GPa from a basement rock with $\mu_2 = 30$ GPa; the crack extends from 1 to 13 km depth and the stress drop is 1 MPa in layer 1 and 3 MPa in medium 2. The displacement computed from the layered model appears to be very close to that computed from a homogeneous model with $\mu_1 = \mu_2 = 30$ GPa and $\Delta\sigma_1 = \Delta\sigma_2 = 3$ MPa. The layered model provides a narrower concentration of the displacement field near the fault strike, which might be accounted for by employing a slightly different fault geometry in the homogeneous crack model.

DISCUSSION AND CONCLUSIONS

A method has been presented to obtain pointwise convergent solutions for antiplane crack problems in layered media. Expansions of dislocation densities in Legendre polynomials provide very accurate solutions for the displacement and stress fields even over the crack surface and at layer discontinuities. As a corollary, a stress-drop discontinuity condition has been obtained, which has a simple interpretation in terms of the welded boundary condition at the interface between different layers. Numerical results show that layering is responsible for significant effects on the stress field, but minor effects are seen in the strain field, provided that the stress-drop discontinuity condition (57) holds, according to which $\frac{\Delta\sigma_1}{\Delta\sigma_2} = \frac{\mu_1}{\mu_2}$.

The stress-drop discontinuity condition has considerable influence on the style of faulting along a transform margin. It is related to the superabundance of boundary conditions that would be prescribed over the fault plane if the stress drop were assigned arbitrarily once the welded boundary condition of continuous slip is already assumed (in order to have a unique solution we may state either tractions or displacement, but not both). At first sight, this condition might appear to be physically sound since, if the two media were deformed by any strain process, starting from a common reference configuration (in which stress and strain both vanish), the component σ^0_{xy}, present before crack slip in an elastic layered medium, must be proportional to the local rigidity value (since the shear strain $\frac{1}{2}(\frac{\partial u^0_y}{\partial x} + \frac{\partial u^0_x}{\partial y})$ must be continuous across a welded interface, even without assuming an antiplane configuration). Accordingly, if the residual stress σ^{r}_{xy} vanishes, the stress drop will obey eq. (57). This is not the case if the residual stress does not vanish, but we might argue that, in a repetitive earthquake cycle, the common reference configuration for both media is one in which the residual stress σ^{r}_{xy}, left by previous earthquakes, is present on the fault plane and subsequent deviatoric deformation generates incremental stresses proportional to the local rigidity values; in the next earthquake

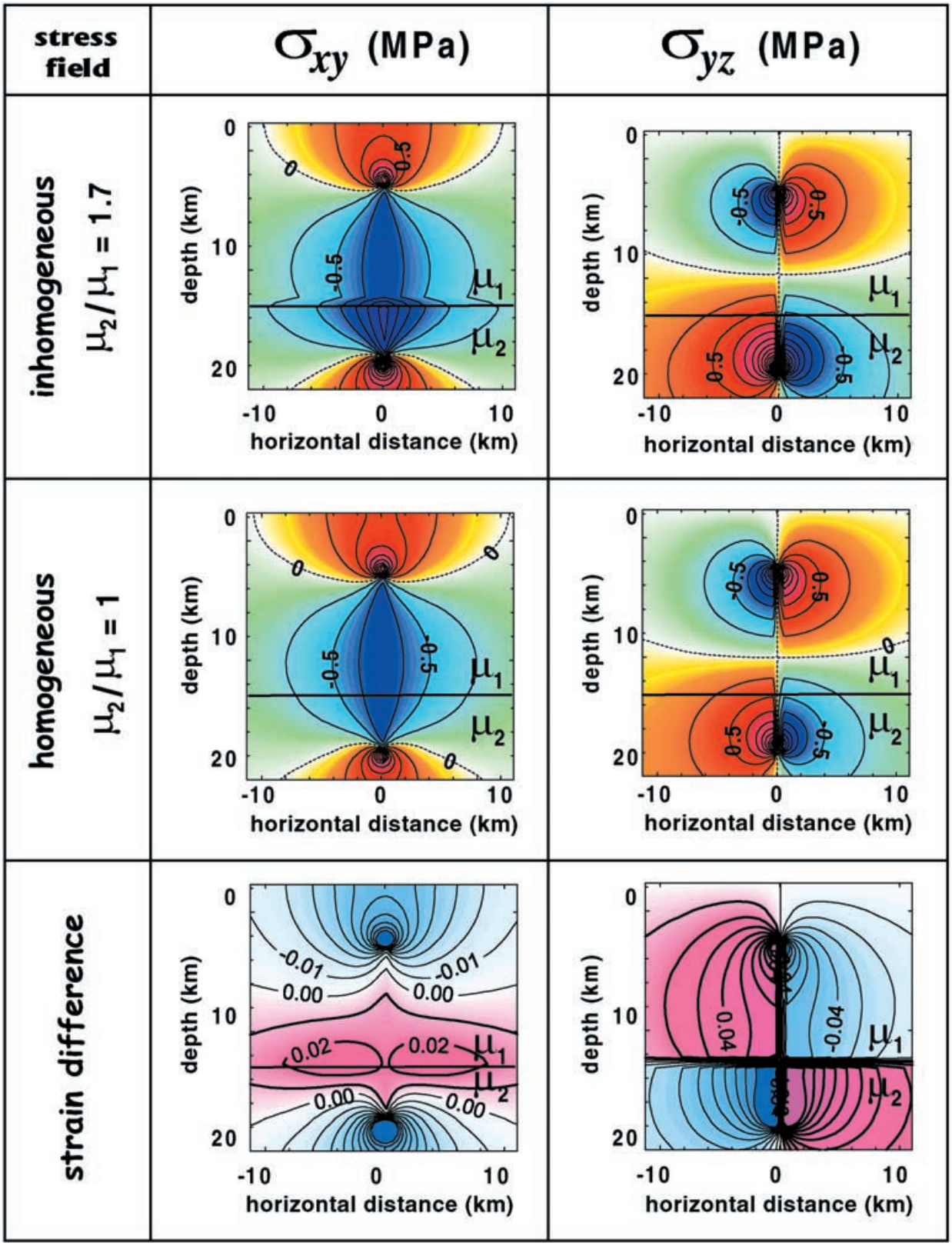

Figure 8. Non-vanishing stress components σ^{c}_{xy} (a) and σ^{c}_{yz} (b), computed for a layered medium with $H = 15$ km, $\mu_2 = 44.1$ GPa, $\mu_1 = \mu_2/1.7 = 26$ GPa. A shear crack complying with the stress drop discontinuity condition ($\Delta\sigma_1 = 1$ MPa and $\Delta\sigma_2 = 1.7$ MPa) extends from $z = 5$ km to $z = 20$ km. For comparison, solutions pertinent to a homogeneous medium, with $\mu_1 = \mu_2 = 26$ GPa and $\Delta\sigma_1 = \Delta\sigma_2 = 1$ MPa are shown in (c) and (d). A horizontal line shows the depth $H = 15$ km. In panels (a)–(d) the distance between iso-lines is 0.25 MPa, positive values are shown from yellow to red, negative values from green to violet. In (e) and (f) the strain difference between the heterogeneous and the homogeneous models are shown. Strain values are normalized to $\Delta\sigma/\mu = 3.85 \times 10^{-5}$. The distance between isolines in panels (e) and (f) is 0.01 MPa. Positive values are in red, negative values in blue.

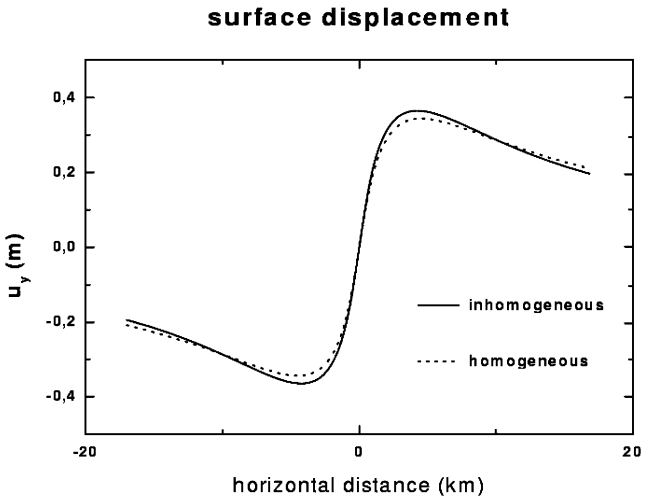

Figure 9. Displacement at the free surface $z = 0$ versus distance from the fault strike x computed for a crack model with $c_1 = 3$ km, $\ell_1 = 2$ km, $c_2 = 9$ km, $\ell_2 = 4$ km, with $H = 5$ km. Rigidity values: $\mu_1 = 10$ GPa, $\mu_2 = 30$ GPa. Stress drop values: $\Delta\sigma_1 = 1$ MPa, $\Delta\sigma_2 = 3$ MPa. The dashed line shows results for a homogeneous model with $\mu_1 = \mu_2 = 30$ GPa and $\Delta\sigma_1 = \Delta\sigma_2 = 3$ MPa.

then, stress drop values complying with eq. (57) will bring the residual stress back to its reference value σ^{r}_{xy}. In a repetitive earthquake cycle, faulting may take place over one planar crack surface across the interface, as described in case C (Figs 7–9). The present model, including the stress drop discontinuity condition, describes accordingly strike-slip faulting events in mature transform faults taking place through brittle and elastic layered media.

Nevertheless, there are several important cases in which the stress-drop discontinuity cannot be satisfied; some of these (the list may be incomplete) are considered in the following.

(1) Fresh fractures developing in the presence of friction: the initial stress in the two media on both sides of the interface is proportional to the local rigidity value, and the residual stress is governed by friction. According to the simplest constitutive relation (Amonton's law), the residual stress is $\sigma^{\mathrm{r}} = f|\sigma_{\mathrm{n}}|$, where f is the friction coefficient and σ_{n} is the $\widehat{xx}$ component of the effective normal stress; σ_{n} is dominated by the lithostatic pressure $\sigma_{\mathrm{n}} = -p_{\mathrm{L}} + p_{\mathrm{w}}$ ($p_{\mathrm{L}} = \int \rho g\, dz$ is the lithostatic pressure and p_{w} is the pore pressure); p_{L} is clearly continuous across the interface and, according to Darcy's law, p_{w} must also be (unless the interface is impervious). Moreover, f is nearly independent of rock type (e.g. Byerlee 1977) and, even according to a more recent formulation of frictional laws (e.g. Scholz 1990), the residual stress is governed by fault rheology, which is independent of rigidity. In such a case, the stress drop cannot obey eq. (57): it may even be negative in a low-rigidity layer (where σ^0_{xy} is lower than σ^{r}) and positive in a high-rigidity layer; similarly, it can be positive in an impervious layer where the pore pressure may be near-lithostatic and negative in a pervious layer where the pore pressure is typically near-hydrostatic (e.g. Rybicki & Yamashita 1998).

(2) Faults developing from a reference configuration in which the stress does not vanish simultaneously in both media: there are a few instances in which σ^0_{xy} prior to crack failure is not proportional to rigidity. Among these, the recent emplacement of sediments or volcanics on top of pre-stressed basement rock is particularly relevant in geophysics. In such cases, the stress drop in the sedimentary layer can be much lower than prescribed by the stress drop discontinuity condition (57).

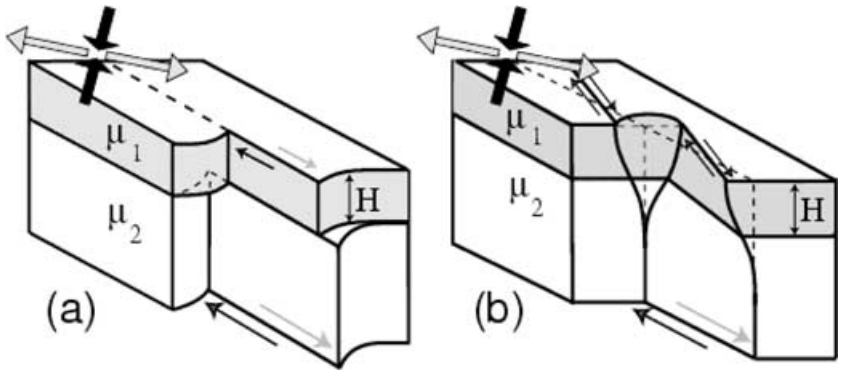

Figure 10. (a) Unwelding of the interface would allow a planar crack, violating the stress-drop discontinuity condition (eq 57), to extend across the interface $z = H$. (b) Non-planar fault surfaces and en-echelon surface ruptures may result when the stress drop in the softer layer is lower than predicted by eq. (57): the stress drop in the softer layer is increased by lowering the residual stress, the stress drop in the harder layer is decreased by increasing the normal stress.

(3) Faults developing across a rheological discontinuity: the stress in a ductile layer is not proportional to strain. For instance, if layer 2 is Maxwell viscoelastic (with instantaneous rigidity μ_2 and effective viscosity η), the initial stress in the brittle layer 1 (with rigidity μ_1) is typically much higher than in the ductile layer 2, even if the instantaneous rigidity in the ductile layer is higher than in the brittle layer; for instance, if a uniform tectonic strain rate $\dot{\epsilon}_{xy}$ is applied at $t = 0$, we have

$$\sigma^0_{\text{brittle}} = \mu_1 \dot{\epsilon} t, \quad \sigma^0_{\text{Maxwell}} = \eta \dot{\epsilon} \left[1 - \mathrm{e}^{-(\mu_2/\eta)t}\right].$$

In this case the stress drop in the softer layer 1 would be much higher than in the harder (coseismically) but ductile medium 2; the stress drop discontinuity condition (57) cannot be fulfilled in a fault event penetrating through the interface.

In all the previous cases, the condition (57) cannot be satisfied and we must conclude that strike-slip faulting cannot be described by crack models within the framework of case C. In all cases except the last, one planar fault may develop across the interface in the long term, after a repetitive earthquake cycle has set on, but in the last case stress relaxation in the harder ductile medium may keep the initial stress lower than in the softer brittle medium forever (if the viscosity is low enough).

One possible way out of this apparent paradox is that the crack does not penetrate across the interface: rock failure might be accomplished as a diffuse deformation near the interface, or the crack may become arrested at the interface, or else an anelastic bulk deformation may prevail in the ductile layer of case 3 above. However, if we maintain that crack models provide physically sound representations of faulting across layered media, we must conclude that the failure of model C must be caused by a violation of one of the assumptions of the model: more specifically, we must admit that:

(1) the interface cannot remain welded during crack slip (see, e.g. Fig. 10a), or
(2) the fault surface cannot be planar (see, e.g. Fig. 10b).

The first possibility entails that a horizontal shear crack develops along the interface $z = H$, as sketched in Fig. 10(a). This may be considered as a particular case of fault branching, leading to horizontal delamination of the fault zone if a suitably high shear component σ_{yz} is present to unweld the interface. In such a case the slip continuity condition (52) is no longer applicable, while condition (53) still holds.

The second possibility entails that the strike direction may be different in the two media as sketched in Fig. 10(b), or the dip of the fault surface cannot be vertical in both media or else that fault branching may take place on one side of the interface.

In-field evidence actually shows that strike-slip faulting at depth is often accompanied by near-surface segmentation of the fault plane into several, en-echelon branches (e.g. Smith & Wyss 1968; Sharp 1976; Tsuneishi *et al.* 1978; Deng & Zhang 1984; Deng *et al.* 1986; Sharp *et al.* 1989; Bjarnason *et al.* 1993). These secondary faults may represent the branching and upward continuation of the main fault (e.g. Segall & Pollard 1980). Detailed study and modelling of surface ruptures indicate that layering and frictional processes largely control the complex surface pattern of faulting in the South Iceland Seismic Zone (Bjarnason *et al.* 1993; Belardinelli *et al.* 2000). Laboratory experiments with clay cakes or sand boxes also suggest the same complex style of fracture (e.g. Tchalenko 1970; Wilcox *et al.* 1972; Naylor *et al.* 1986; Mandl 1988) in which 'Riedel shears' with plough-share shape depart upward from a planar basement fault, during the early stages of faulting. Only after prolonged slip, does a throughgoing fault with the same strike as the basement fault develop in the shallow layer, in agreement with the considerations made above for a repetitive earthquake cycle.

Moreover, faulting above a wide zone of basement wrenching (similar to the ductile layer of case 3 above) is observed to be accompanied by antithetic faulting in the conjugate direction. In-field evidence of similar mechanisms are present in several areas of the world, where deep shear movements manifest as bookshelf faulting near the surface (for a review see Wilcox *et al.* 1972). One similar case is the South Iceland Seismic Zone (SISZ), located between the eastern and western rift zones of Iceland. Large strike-slip earthquakes have occurred there in the recent past (two $M_s = 6.6$ earthquakes took place in 2000 June), with magnitudes up to 7 and an interevent time of approximately 80 yr. GPS measurements show that the SISZ is undergoing left lateral shear in the ENE–WSW direction at a rate of 2 cm yr^{-1}. However, major earthquakes in the SISZ do not take place on similarly trending sinistral faults but on N–S trending, dextral faults. These faults are normally steeply dipping, the measured horizontal displacement ranges from 1 m to >15 m: the SISZ appears to be a transform zone under formation (Bjarnason *et al.* 1993), the origin of which can be ascribed to the southward migration of the Eastern rift zone.

In conclusion, several pieces of evidence show that planar fault surfaces across layered media may develop along a transform margin only when the stress-drop discontinuity condition is satisfied; when this condition cannot be satisfied for a planar fault, a complex pattern of faulting develops, in which 3-D geometries are necessarily involved: these include twisting, bending and multiple branching of the basement fault. Finally, even if laboratory experiments show that one planar fault may develop in the mature stage of a transform margin, it is difficult to believe that a mature fault system in the field can maintain a perfectly matching stress drop discontinuity eq. (57), since the stress drop over a slipping fault is mostly governed by fault rheology, which is independent of rigidity layering. Thus we may conclude that geometrical complexities must accompany faulting across heterogeneous media even in mature fault systems.

ACKNOWLEDGMENTS

Useful comments and suggestions by A. Del. Ben, K. R. Rybicki, T. Yamashita, R. Madariaga and F. Pollitz are gratefully acknowledged. Work performed with financial contribution from MURST and from the Commission of European Communities (Program Environment and Climate, project PRENLAB-2). E.R. was supported by a C.E.C. fellowship under contract ENV4-CT97-0536.

REFERENCES

Abramowitz, M. & Stegun, I.A., 1964. *Handbook of Mathematical Functions,* Dover, New York.

Antonioli, A., Piersanti, A. & Spada, G., 1998. Stress diffusion following large strike-slip earthquakes, *Geophys. J. Int.,* **133,** 85–90.

Belardinelli, M.E., Bonafede, M. & Gudmundsson, A., 2000. Secondary earthquake fractures generated by a strike-slip fault in the South Iceland seismic zone, *J. geophys. Res.,* **105,** 13 613–13 630.

Ben-Zion, Y., 1990. The response of two half-spaces to point dislocations at the material interface, *Geophys. J. Int.,* **101,** 507–528.

Bjarnason, I., Cowie, P., Anders, M.H., Seeber, L. & Scholz, C.H., 1993. The 1912 Iceland earthquake rupture: growth and development of a nascent transform system, *Bull. seism. Soc. Am.,* **83,** 416–435.

Bonafede, M. & Rivalta, E., 1999a. On tensile cracks close to and across the interface between two welded elastic half-spaces, *Geophys. J. Int.,* **138,** 410–434.

Bonafede, M. & Rivalta, E., 1999b. The tensile dislocation problem in a layered medium, *Geophys. J. Int.,* **136,** 341–356.

Bonafede, M., Dragoni, M. & Boschi, E., 1985. Quasi-static crack models and the frictional stress threshold criterion for slip arrest, *Geophys. J. R. astr. Soc.,* **83,** 615–635.

Byerlee, J.D., 1977. Friction of rocks, in *Experimental Studies of Rock Friction with Application to Earthquake Prediction,* pp. 55–77, ed. Evernden, J.F., US Geological Survey, Menlo Park, CA.

Davis, K.T.R. & Davis, R.W., 1989. Evaluation of a class of integrals occurring in mathematical physics via a higher order generalization of the principal value, *Can. J. Phys.,* **67,** 759–765.

Deng, Q. & Zhang, P., 1984. Research on the geometry of shear fracture zones, *J. geophys. Res.,* **89,** 5699–5710.

Deng, Q., Wu, D., Zhang, P. & Chen, S., 1986. Structure and deformational character of strike-slip fault zones, *Pure appl. Geophys.,* **124,** 204–223.

Erdogan, F., Gupta, G.D. & Cook, T.S., 1973. Numerical solution of singular integral equations, in, *Mechanics of Fracture,* Vol. 1, Sih, G.C. Noordhoff, Leyden.

Fung, Y.C., 1965. *Foundation of Solid Mechanics,* Prentice-Hall, Englewood Cliffs, NJ.

Gomberg, J., Beeler, N.M., Blanpied, M.L. & Bodin, P., 1998. Earthquake triggering by transient and static deformation, *J. geophys. Res.,* **103,** 24 411–24 426.

Gradshteyn, I.S. & Ryzhik, I.M., 1965. *Tables of Integral Series and Products,* 4th edn, Academic Press, New York.

Harris, R.A., 1998. Introduction to special section: stress triggers, stress shadows and implications for seismic hazard, *J. geophys. Res.,* **103,** 24 347–24 358.

Harris, R.A. & Simpson, R.W., 1998. Suppression of large earthquakes by stress shadows: a comparison of Coulomb and rate-state failure, *J. geophys. Res.,* **103,** 24 439–24 452.

Kagan, Y.Y. & Jackson, D.D., 1998. Spatial aftershock distribution: effect of normal stress, *J. geophys. Res.,* **103,** 24 453–24 468.

King, G.C.P., Stein, R.S. & Lin, J., 1994. Static stress change and the triggering of earthquakes, *Bull. seism. Soc. Am.,* **84,** 935–953.

Kumari, G., Singh, S. & Singh, K., 1992. Static deformation of two welded elastic half-spaces caused by a point dislocation source, *Phys. Earth planet. Inter.,* **73,** 53–76.

Ma, X. & Kusznir, N., 1994. Coseismic and postseismic subsurface displacements and strains for a vertical strike-slip fault in a three layer elastic medium, *Pageoph,* **142,** 687–709.

Mandl, G., 1988. *Mechanics of tectonic faulting,* Elsevier, Amsterdam.

Morelli, A., Bonafede, M. & Dragoni, M., 1987. Two dimensional crack model of faulting in a layered elastic half space, *Ann. Geophys.,* **5B,** 281–288.

Muskhelishvili, N.I., 1953. *Singular Integral Equations,* P. Noordhoff, Groningen, The Netherlands.

Nalbant, S.S., Hubert, A. & King, G.C.P., 1998. Stress coupling between earthquakes in northwest Turkey and the north Aegean sea, *J. geophys. Res.,* **103,** 24 469–24 486.

Naylor, M.A., Mandl, G. & Sijpestein, C.H.K., 1986. Fault geometries in basement-induced wrench faulting under different initial stress states, *J. Struct. Geol.,* **7,** 737–752.

Okada, Y., 1992. Internal deformation due to shear and tensile faults in a half-space, *Bull. seism. Soc. Am.,* **82,** 1018–1040.

Perfettini, H., Stein, R.S., Simpson, R.W. & Cocco, M., 1999. Stress transfer by the 1988–1989 $M = 5.3$ and 5.4 Lake Elsman foreshocks to the Loma Prieta Fault: unclamping at the site of peak mainshock slip, *J. geophys. Res.,* **104,** 20 169–20 182.

Piersanti, A., Spada, G., Sabadini, R. & Bonafede, M., 1995. Global postseismic deformation, *Geophys. J. Int.,* **120,** 544–566.

Piersanti, A., Spada, G. & Sabadini, R., 1997. Global post-seismic rebound of a viscoelastic Earth: theory for finite faults and application to the 1964 Alaska earthquake, *J. geophys. Res.,* **102,** 477–492.

Pollitz, F.F., 1992. Postseismic relaxation theory on the spherical earth, *Bull. seism. Soc. Am.,* **82,** 422–453.

Pollitz, F.F. & Sacks, I.S., 1996. Viscosity structure beneath northeast Iceland, *J. geophys. Res.,* **101,** 17 771–17 793.

Rani, S., Singh, S. & Kumari, G., 1995. Static deformation of two welded elastic half-spaces caused by rectangular shear fault located on the interface, *Phys. Earth planet. Inter.,* **92,** 261–269.

Rivalta, E., Mangiavillano, W. & Bonafede, M., 2002. The edge dislocation problem in a layered elastic medium, *Geophys. J. Int.,* in press.

Roth, F., 1990. Subsurface deformations in a layered half-space, *Geophys. J. Int.,* **103,** 147–155.

Rundle, J.B., 1978. Viscoelastic crustal deformation by finite quasi-static sources, *J. geophys. Res.,* **83,** 5937–5945.

Rybicki, K.R., 1971. The elastic residual field of a very long strike-slip fault in the presence of a discontinuity, *Bull. seism. Soc. Am.,* **61,** 79–92.

Rybicki, K.R., 1973. Analysis of aftershocks on the basis of dislocation theory, *Phys. Earth planet. Inter.,* **7,** 409–422.

Rybicki, K.R. & Yamashita, T., 1998. Faulting in vertical inhomogeneous media and its geophysical implications, *Geophys. Res. Lett.,* **25,** 2893–2896.

Savage, J.C., 1987. Effests of crustal layering upon dislocation modelling, *J. geophys. Res.,* **92,** 10 595–10 600.

Savage, J.C., 1998. Displacement field for an edge dislocation in a layered half-space, *J. geophys. Res.,* **103,** 2439–2446.

Scholz, C.H., 1990. *The Mechanics of Earthquake and Faulting,* Cambridge University Press, Cambridge.

Segall, P. & Pollard, D.D., 1980. Mechanics of discontinuous faults, *J. geophys. Res.,* **85,** 4337–4350.

Sharp, R.V., 1976. Surface faulting in Imperial Valley during the earthquake swarm of January–February 1975, *Bull. seism. Soc. Am.,* **66,** 1145–1154.

Sharp, R.V. *et al.*, 1989. Surface faulting along the Superstition Hills fault zone and nearby faults, associated to the earthquake of 24 November 1987, *Bull. seism. Soc. Am.,* **79,** 252–281.

Singh, S.J., 1970. Static deformation of a multilayered half-space by internal sources, *J. geophys. Res.,* **75,** 3257–3263.

Singh, S., Kumari, G. & Singh, K., 1993. Static deformation of two welded elastic half-spaces caused by a finite rectangular fault, *Phys. Earth planet. Inter.,* **97,** 313–333.

Smith, S.W. & Wyss, M., 1968. Displacement on the San Andreas fault subsequent to the 1966 Parkfield earthquake, *Bull. seism. Soc. Am.,* **58,** 1955–1973.

Stein, R.S., King, G.C.P. & Lin, J., 1992. Change in failure stress on the southern San Andreas fault system caused by the 1992 magnitude = 7.4 Landers earthquake, *Science,* **258,** 1328–1332.

Tchalenko, J.S., 1970. Similarities between shear zones of different magnitudes, *Bull. seism. Soc. Am.,* **81,** 1625–1640.

Tinti S. & Armigliato, 1998. Displacement and stresses induced by a point source across a plane interface separating two elastic semi-infinite spaces: an analytical solution, *J. geophys. Res.,* **103,** 15 109–15 125.

Tsuneishi, Y., Ito, T. & Kano, K., 1978. Surface faulting associated with the

1978 Izu-Oshima-kinkai earthquake, *Bull. Earthq. Res. Inst., Univ. Tokyo,* 649–672.

Wilcox, R.E., Harding, T.P. & Seely, D.R., 1972. Basic wrench tectonics, *Am. Assoc. Petrol. Geol. Bull.,* **57,** 74–96.

APPENDIX A: EVALUATING THE INTEGRALS I_1 AND I_2 (CASES A AND B)

We compute here integrals I_1, eq. (25), and I_2, eq. (26), for cases A and B, employing the following change of variables, being $|\xi'| \leq 1$ and $|\xi| \leq 1$.

$$\begin{aligned} \xi &= \cos\varphi \\ \xi' &= \cos\theta. \end{aligned} \tag{A1}$$

By applying eq. (A1) and the definition of Chebyshev polynomials, the integral $I_1(k, i)$ can be written as

$$I_1(k,i) = \frac{1}{4}\int_{-\pi}^{\pi} \sin[(i+1)\varphi]\sin\varphi\, d\varphi \int_{-\pi}^{\pi} \frac{\cos k\theta}{\cos\theta + \cos\varphi + 2(\lambda - h)}\, d\theta, \tag{A2}$$

Let us define

$$\alpha = \cos\varphi + 2(\lambda - h). \tag{A3}$$

In case A, $\alpha > 1\, \forall\varphi \in [-\pi, \pi]$ since $\lambda - h > 1$ while, in case B, $\alpha = 1$ in $\varphi = \pm\pi$. We define

$$R_\alpha = \int_{-\pi}^{\pi} \frac{\cos k\theta}{\cos\theta + \alpha}\, d\theta = 2\Im \oint_{C_1} \frac{z^k}{(z - z_1)(z - z_2)}\, dz, \tag{A4}$$

where C_1 is the unit circle in the complex plane, $z = \mathrm{e}^{i\theta}$ and the simple poles of integrand function are

$$\begin{aligned} z_1 &= -\alpha + \sqrt{\alpha^2 - 1} \\ z_2 &= -\alpha - \sqrt{\alpha^2 - 1}. \end{aligned}$$

In case A, only z_1 is within the integration path since $\alpha > 1$. Then, employing the Theorem of Residues, R_α is computed analytically as

$$R_\alpha = 2\pi \frac{(-\alpha + \sqrt{\alpha^2 - 1})^k}{\sqrt{\alpha^2 - 1}}.$$

Introducing R_α in eq. (A2) we obtain

$$I_1(k,i) = \frac{\pi}{2}\int_{-\pi}^{\pi} \sin[(i+1)\varphi]\sin\varphi \frac{(-\alpha + \sqrt{\alpha^2 - 1})^k}{\sqrt{\alpha^2 - 1}}\, d\varphi. \tag{A5}$$

This integral can be computed efficiently employing a Gauss–Chebyshev quadrature formula. In case B, $\alpha > 1$ as far as $\varphi \neq \pm\pi$ (so that the same formula obtained above for R_α still holds) but $\alpha = 1$ when $\varphi = \pm\pi$ (then R_α is unbounded): in this case $z_1 = z_2 = -1$ and the two poles cohalesce into a double pole on the integration path. Then, R_α can still be computed as the Residual principal value (Davis & Davis 1989), but we may also rewrite the product $\sin\varphi/(\alpha^2 - 1)^{1/2}$ appearing in eq. (A5) as $(1 - \cos\varphi)^{1/2}/(3 + \cos\varphi)^{1/2}$ which is bounded in $\varphi = \pm\pi$: after employing this simplification in eq. (A5), $I_1(k, i)$ can be computed efficiently even in case B.

In much the same way as shown for $I_1(k, i)$, the integration with respect to ξ' (i.e. θ) appearing in I_2 can be performed, yielding

$$I_2(k,i,n) = \frac{\pi}{2}\int_{-\pi}^{\pi} \sin[(i+1)\varphi]\sin\varphi \frac{\left(-\beta_n + \sqrt{\beta_n^2 - 1}\right)^k}{\sqrt{\beta_n^2 - 1}}\, d\varphi, \tag{A6}$$

where $\beta_n = \cos\varphi + 2(\lambda + nh)$. Since $\beta_n > 1$, the integrand above is bounded both in cases A and B and $I_2(k, i, n)$ can be computed efficiently employing a Gauss–Chebyshev quadrature formula.

APPENDIX B: SINGULAR BEHAVIOUR OF THE DISLOCATION DENSITY

In this Appendix, the system (40), leading to the supplementary conditions (43) and (44) for case C, will be derived. As a particular case, eq. (36) for case B can be obtained by letting $\rho_1 = 0$. To this end, we generalize to our system of coupled eqs (40) the method proposed by Erdogan *et al.* (1973). From now on, variable t will denote either ξ_1' or ξ_2' and ξ will denote either ξ_1 or ξ_2. The equilibrium equations (40) can be rewritten as

$$\begin{aligned} -\frac{2\pi}{\mu_1}\Delta\sigma_1(\xi) &= \int_{-1}^{1}\left\{\frac{\rho_1(t)}{t-\xi} + b_0\frac{\rho_1(t)}{t - z_1(\xi)} + c_0\frac{\rho_2(-t)}{t - \hat{z}_1(\xi)}\right\} dt - \int_{-1}^{1}\rho_1(t)\mathcal{R}_{11}(\xi,t)\, dt - \int_{-1}^{1}\rho_2(t)\mathcal{R}_{12}(\xi,t)\, dt \\ -\frac{2\pi}{\mu_2}\Delta\sigma_2(\xi) &= \int_{-1}^{1}\left\{\frac{\rho_2(t)}{t-\xi} + b_0'\frac{\rho_2(t)}{t - z_2(\xi)} + c_0'\frac{\rho_1(-t)}{t - \hat{z}_2(\xi)}\right\} dt - \int_{-1}^{1}\rho_1(t)\mathcal{R}_{21}(\xi,t)\, dt + \int_{-1}^{1}\rho_2(t)\mathcal{R}_{22}(\xi,t)\, dt, \end{aligned} \tag{B1}$$

where $z_1 = 1 + (1-\xi)\,e^{i\theta_1}$, $\hat{z}_1 = 1 + \ell_1/\ell_2(1-\xi)\,e^{i\hat{\theta}_1}$ are points of the complex plane on oriented segments L_1 and $\hat{L}_1$ with origin in $\xi = 1$ and orientation $\theta_1 = \hat{\theta}_1 = 0$; $z_2 = -1 + (1+\xi)\,e^{i\theta_2}$ and $\hat{z}_2 = -1 + \ell_2/\ell_1(1+\xi)\,e^{i\hat{\theta}_2}$, instead, are points of the complex plane on segments L_2 and $\hat{L}_2$ with origin in $\xi = -1$ and orientation $\theta_2 = \hat{\theta}_2 = \pi$. Integral kernels $\mathcal{R}_{11}, \mathcal{R}_{12}, \mathcal{R}_{21}$ and $\mathcal{R}_{22}$ are written in eq. (40); constants b_0, c_0, b_0', c_0' are the following in terms of $m = \mu_2/\mu_1$:

$$b_0 = \frac{1-m}{1+m} \qquad b_0' = -\frac{1-m}{1+m}$$
$$c_0 = -\frac{2m}{1+m} \quad c_0' = -\frac{2}{1+m}. \tag{B2}$$

Following Muskhelishvili (1953) it is possible to obtain the asymptotic behaviour of different terms in eq. (B1). Consider the first integral in the right-hand side of the first eq. (B1). After inserting the expressions (42) for ρ_1 and ρ_2, let us study the following function $\Phi(\zeta)$ of the complex variable $\zeta = \xi + i\eta$:

$$\Phi(\zeta) = \frac{1}{2\pi i}\int_{-1}^{1}\frac{\rho_1(t)}{t-\zeta}\,dt = \frac{1}{2\pi i}e^{-i\pi a_1}\int_{-1}^{1}\frac{R_1(t)\,(t-1)^{a_1}(t+1)^{b_1}}{t-\zeta}\,dt. \tag{B3}$$

The asymptotic behaviour of $\Phi(\zeta)$ near $\zeta = \pm 1$ can be estimated; if $a_1 < 0$ and $b_1 < 0$ then $\Phi(\zeta)$ can be written as

$$\Phi(\zeta) = -R_1(-1)2^{a_1}\frac{e^{-i\pi b_1}}{2i\sin\pi b_1}(\zeta+1)^{b_1} + R_1(1)2^{b_1}\frac{(\zeta-1)^{a_1}}{2i\sin\pi a_1} + \Phi_0(\zeta), \tag{B4}$$

where $\Phi_0(\zeta)$ is bounded everywhere, with the only possible exception of $\zeta = \pm 1$ where its order of infinity is less then either a_1 or b_1. If $a_1 = 0$ or $b_1 = 0$, logarithmic singularities $\ln(\zeta+1)$ or $\ln(\zeta-1)$ are obtained instead of the algebraic singularities $(\zeta+1)^{b_1}$ or $(\zeta-1)^{a_1}$, and the following arguments still hold with only minor changes.

If $\zeta = \xi \in (-1, +1)$ (on the cut), by using the Plemelij formula:

$$\frac{1}{2\pi i}\int_{-1}^{1}\frac{\rho(t)}{t-\xi}\,dt = \frac{1}{2}[\Phi^+(\xi) + \Phi^-(\xi)] \tag{B5}$$

we obtain the following evaluation of the first term on the right-hand side of eq. (B1):

$$\frac{1}{\pi}\int_{-1}^{1}\frac{\rho_1(t)}{t-\xi}\,dt = -R_1(-1)2^{a_1}\cot\pi b_1(\xi+1)^{b_1} + R_1(1)2^{b_1}\cot\pi a_1(1-\xi)^{a_1} + F_0(\xi). \tag{B6}$$

The behaviour of $F_0(\xi)$ is similar to that of Φ_0.

Let us now consider the second integral in the former of eq. (B1). Letting $\zeta = z_1$ in eq. (B3), the obtained function is olomorphic everywhere on L_1, apart from $z_1 = 1$; substituting z_1 in eq. (B4) it follows that

$$\Phi(z_1) = R_1(1)2^{b_1}\frac{(1-\xi)^{a_1}}{2i\sin\pi a_1} + F_1(\xi), \quad -1 < \xi < 1. \tag{B7}$$

The behaviour of $F_1(\xi)$ is similar to that described above for F_0 and Φ_0. The last equality represents, if multiplied by a factor of $2ic_0$, the second integral of the first eq. (B1). In a similar way the third integral can be evaluated from its corresponding function $\Phi(\hat{z}_1)$:

$$\Phi(\hat{z}_1) = R_2(-1)2^{a_2}\left[\frac{\ell_1}{\ell_2}(1-\xi)\right]^{b_2}\frac{1}{2i\sin\pi b_2} + \hat{F}_1(\xi), \quad -1 < \xi < 1. \tag{B8}$$

Then, substituting eqs (B6)–(B8) in the former of eq. (B1) yields

$$-\frac{2}{\mu_1}\Delta\sigma_1 = -R_1(-1)2^{a_1}\cot\pi b_1(\xi+1)^{b_1} + R_1(1)2^{b_1}\cot\pi a_1(1-\xi)^{a_1} + b_0R_1(1)2^{b_1}\frac{(1-\xi)^{a_1}}{\sin\pi a_1}$$
$$+ c_0R_2(-1)2^{a_2}\left[\frac{\ell_1}{\ell_2}(1-\xi)\right]^{b_2}\frac{1}{\sin\pi b_2} + F_0(\xi) + F_1(\xi) + \hat{F}_1(\xi) + F_2(\xi), \tag{B9}$$

where $F_2(\xi)$ represents the contribution of the fourth and the fifth terms in the first equation of the system (B1). In the same way the asymptotic evaluation of the second eq. (B1) is obtained:

$$-\frac{2}{\mu_2}\Delta\sigma_2 = -R_2(-1)2^{a_2}\cot\pi b_2(\xi+1)^{b_2} + R_2(1)2^{b_2}\cot\pi a_2(1-\xi)^{a_2} - b_0'R_2(-1)2^{a_2}\frac{(1+\xi)^{b_2}}{\sin\pi b_2}$$
$$- c_0'R_1(1)2^{b_1}\left[\frac{\ell_2}{\ell_1}(1+\xi)\right]^{a_1}\frac{1}{\sin\pi a_1} + G_0(\xi) + G_1(\xi) + \hat{G}_1(\xi) + G_2(\xi). \tag{B10}$$

If we multiply both sides of eq. (B9) by $(1+\xi)^{-b_1}$ and let $\xi \to -1$, we obtain

$$\cot\pi b_1 = 0 \quad \text{i.e.} \quad b_1 = -\frac{1}{2}. \tag{B11}$$

Similarly, if we multiply both sides of eq. (B10) by $(1-\xi)^{-a_2}$ and let $\xi \to 1$, we obtain

$$\cot \pi a_2 = 0 \quad \text{i.e.} \quad a_2 = -\frac{1}{2}. \tag{B12}$$

Multiplying now both sides of eq. (B9) by $(1-\xi)^{-a_1}$ and letting $\xi \to 1$, yields

$$R_1(1)2^{b_1} \cot \pi a_1 + b_0 R_1(1)2^{b_1} \frac{1}{\sin \pi a_1} + c_0 R_2(-1)2^{a_2} \left[\frac{\ell_1}{\ell_2}(1-\xi)\right]^{b_2-a_1} \frac{1}{\sin \pi b_2} = 0 \tag{B13}$$

from which we infer $b_2 \geq a_1$. Multiplying both sides of eq. (B10) by $(1+\xi)^{-b_2}$ and letting $\xi \to -1$ we infer that $a_1 \geq b_2$ so that

$$a_1 = b_2 = \omega. \tag{B14}$$

Employing this result in eqs (B9) and (B10), the two following conditions are obtained for $R_1(1)$ and $R_2(-1)$:

$$R_1(1)\left[\cos \pi\omega + \frac{1-m}{1+m}\right] - \frac{2m}{1+m}\left(\frac{\ell_1}{\ell_2}\right)^{\omega} R_2(-1) = 0 \tag{B15}$$

$$-\frac{2}{1+m}\left(\frac{\ell_2}{\ell_1}\right)^{\omega} R_1(1) + R_2(-1)\left[\cos \pi\omega - \frac{1-m}{1+m}\right] = 0. \tag{B16}$$

Since $R_1(1) \neq 0$ and $R_2(-1) \neq 0$, the determinant of the system formed by eqs (B15) and (B16) must vanish. The order of singularity ω is then determined by the following equation, under the constraint $-1 < \omega \leq 0$:

$$\cos^2 \pi\omega - 1 = 0 \quad \text{i.e.} \quad \omega = 0. \tag{B17}$$

Actually, since we have inferred that $a_1 = \omega = 0$, the asymptotic expression (B4) in proximity of $\zeta = 1$, which is valid for negative exponents, should be changed to

$$\Phi(\zeta) = -R_1(-1)\frac{e^{-i\pi b_1}}{2i \sin \pi b_1}(\zeta+1)^{b_1} + R_1(1)2^{b_1} \log(\zeta-1) + \Phi_0(\zeta) \tag{B18}$$

showing that logarithmic singularities appear from the three singular terms in the equilibrium equation (B1). Similar considerations apply for the asymptotic evaluation of the second equation in eq. (B1) near $\zeta = -1$. The previous arguments, leading to eq. (B15), can be repeated with obvious minor changes, leading to eq. (B15) with $\omega = 0$.

In closing this appendix, it can be mentioned that eq. (36) for case B can be simply obtained by assuming $\rho_1 = 0$ in the second of eq. (B1), i.e. by assuming $R_1(1) = 0$ in eq. (B16).

APPENDIX C: EVALUATING INTEGRALS APPEARING IN EQ. (40)

In this appendix a sketch is given of the method employed in computing the integrals appearing in eq. (40) when the expansions (50) and (47) are inserted for ρ_1 and ρ_2. The first integral to be considered is

$$I_{11}(\xi_1) = \int_{-1}^{1} \frac{1}{t'} \sum_{k=0}^{\infty} b_k P_{2k}(t') \frac{d\xi'}{\xi_1 - \xi'}, \quad \text{with} \quad t' = \sqrt{\frac{1+\xi'}{2}}, \tag{C1}$$

where ξ' is written instead of ξ_1'. Changing the integration variable to t' and posing

$$t_1 = \sqrt{\frac{1+\xi_1}{2}}, \tag{C2}$$

yields

$$I_{11}(\xi_1) = 2\sum_{k=0}^{\infty} b_k \int_0^1 \frac{P_{2k}(t')\,dt'}{t_1^2 - t'^2} = \sum_{k=0}^{\infty} \frac{b_k}{t_1}\left(\int_0^1 \frac{P_{2k}(t')\,dt'}{t_1 - t'} + \int_0^1 \frac{P_{2k}(t')\,dt'}{t_1 + t'}\right). \tag{C3}$$

Changing t' to $t'' = -t'$ in the second integral and rewriting $P_{2k}(-t'') = P_{2k}(t'')$ we obtain

$$I_{11}(\xi_1) = \sum_{k=0}^{\infty} \frac{b_k}{t_1} \int_{-1}^{1} \frac{P_{2k}(t')\,dt'}{t_1 - t'} = \frac{2}{t_1} \sum_{k=0}^{\infty} b_k Q_{2k}(t_1), \tag{C4}$$

where $Q_k(t)$ are Legendre function of the second kind, which have logarithmic singularities in $t = \pm 1$. These may be written for a complex argument z as

$$Q_{2k}(z) = \frac{1}{2} P_{2k}(z) \ln \frac{z+1}{z-1} - W_{2k-1}(z), \quad \text{with} \quad W_{2k-1}(z) = \sum_{n=1}^{2k} \frac{1}{n} P_{n-1}(z) P_{2k-n}(z). \tag{C5}$$

If z is real and $|z| < 1$, the absolute value of the argument of the logarithmic term is to be taken (e.g. Gradshteyn & Ryzhik 1965). In much the same way, the singular integrals I_{12}, I_{13}, I_{21}, I_{22}, I_{23} can be computed, obtaining the results shown in eq. (55).

Let us consider now the integral containing the regular kernel $\mathcal{R}_{11}$ in eq. (40). This may be written as (with terms having their obvious meanings)

$$I_{14}(\xi_1) = \sum_{k=0}^{\infty} b_k \left\{ J_0(k) + \sum_{n=1}^{\infty} \Gamma^n [J_1(n,k) + J_2(n,k) + J_3(n,k) + \Gamma J_4(n,k)] \right\}. \tag{C6}$$

Taking into account that $h_1 > 2$ and proceeding as above (employing complex arguments when necessary), we obtain

$$\begin{aligned}
J_0(k) &= \int_0^1 \frac{4P_{2k}(t')\,dt'}{\xi' + \xi_1 + 2h_1 - 2} = -\frac{2}{i w_0} Q_{2k}(i w_0) && \text{with} \quad w_0^2 = h_1 - \frac{3-\xi_1}{2} \\
J_1(n,k) &= \int_0^1 \frac{4P_{2k}(t')\,dt'}{\xi' - \xi_1 - 2nh_1} = -\frac{2}{w_1} Q_{2k}(w_1) && \text{with} \quad w_1^2 = nh_1 + \frac{1+\xi_1}{2} \\
J_2(n,k) &= \int_0^1 \frac{4P_{2k}(t')\,dt'}{\xi' - \xi_1 + 2nh_1} = -\frac{2}{i w_2} Q_{2k}(i w_2) && \text{with} \quad w_2^2 = nh_1 - \frac{1+\xi_1}{2} \\
J_3(n,k) &= \int_0^1 \frac{4P_{2k}(t')\,dt'}{\xi' + \xi_1 - 2 + 2(n+1)h_1} = -\frac{2}{i w_3} Q_{2k}(i w_3) && \text{with} \quad w_3^2 = (n+1)h_1 - \frac{3-\xi_1}{2} \\
J_4(n,k) &= \int_0^1 \frac{4P_{2k}(t')\,dt'}{\xi' + \xi_1 - 2 - 2nh_1} = -\frac{2}{w_4} Q_{2k}(w_4) && \text{with} \quad w_4^2 = nh_1 + \frac{3-\xi_1}{2}.
\end{aligned} \tag{C7}$$

In spite of the appearence of imaginary arguments in some of the previous formulae, all these integrals are real-valued since

$$\ln \frac{i w + 1}{i w - 1} = i(2 \arctan w + \pi)$$

and $Q_{2k}(i w)$ is imaginary, according to eq. (C5).

Let us consider now the integral containing the kernel $\mathcal{R}_{12}$ in eq. (40). It may be written as

$$I_{15}(\xi_1) = \frac{2m}{1+m} \sum_{n=0}^{\infty} \left\{ \Gamma^n \sum_{k=0}^{\infty} a_k [J_5(n,k) + \Gamma J_6(n,k)] \right\} \tag{C8}$$

and

$$\begin{aligned}
J_5(n,k) &= \int_0^1 \frac{4P_{2k}(t')\,dt'}{\xi' + \frac{\ell_1}{\ell_2}\xi_1 + 1 - \frac{\ell_1}{\ell_2} + 2(n+1)h_2} = +\frac{2}{w_5} Q_{2k}(w_5) \quad \text{with} \quad w_5^2 = 1 - \frac{\ell_1}{\ell_2}\left(\frac{1-\xi_1}{2}\right) + (n+1)h_2 \\
J_6(n,k) &= \int_0^1 \frac{4P_{2k}(t')\,dt'}{\xi' - \frac{\ell_1}{\ell_2}\xi + 1 + \frac{\ell_1}{\ell_2} + 2(n+1)h_2} = +\frac{2}{w_6} Q_{2k}(w_6) \quad \text{with} \quad w_6^2 = 1 + \frac{\ell_1}{\ell_2}\left(\frac{1-\xi_1}{2}\right) + (n+1)h_2.
\end{aligned} \tag{C9}$$

The integral containing the kernel $\mathcal{R}_{21}$ in eq. (40) can be written as

$$I_{24}(\xi_2) = \sum_{n=0}^{\infty} \Gamma^n \left\{ \sum_{k=0}^{\infty} b_k [J_7(n,k) + \Gamma J_8(n,k)] \right\}, \tag{C10}$$

where

$$\begin{aligned}
J_7(n,k) &= \int_0^1 \frac{4P_{2k}(t')\,dt'}{\xi' - 1 + \frac{\ell_2}{\ell_1}(\xi_2 + 1) + 2(n+1)h_1} = -\frac{2}{i w_7} Q_{2k}(i w_7) \quad \text{with} \quad w_7^2 = -1 + \frac{\ell_2}{\ell_1}\left(\frac{1+\xi_2}{2}\right) + (n+1)h_1 \\
J_8(n,k) &= \int_0^1 \frac{4P_{2k}(t')\,dt'}{\xi' - 1 - \frac{\ell_2}{\ell_1}(\xi_2 + 1) - 2(n+1)h_2} = -\frac{2}{w_8} Q_{2k}(w_8) \quad \text{with} \quad w_8^2 = 1 + \frac{\ell_2}{\ell_1}\left(\frac{1+\xi_2}{2}\right) + (n+1)h_1.
\end{aligned} \tag{C11}$$

Finally, the integral containing the kernel $\mathcal{R}_{22}$ in eq. (40) can be written as

$$I_{25}(\xi_2) = \sum_{n=0}^{\infty} \Gamma^n \left\{ \sum_{k=0}^{\infty} a_k J_9(n,k) \right\}, \tag{C12}$$

where

$$J_9(n,k) = \int_0^1 \frac{4P_{2k}(t')\,dt'}{\xi' + \xi_2 + 2 + 2(n+1)h_2} = +\frac{2}{w_9} Q_{2k}(w_9) \quad \text{with} \quad w_9^2 = \frac{3+\xi_2}{2} + (n+1)h_2. \tag{C13}$$